NAVAL POSTGRADUATE SCHOOL

MONTEREY, CALIFORNIA

THESIS

MARITIME SURVEILLANCE USING A WIDEBAND HYDROPHONE

by

Jason Keith Wilson

September 2007

Thesis Advisor:	Joseph Rice
Co-Advisors:	Daphne Kapolka
	Paul Hursky

Approved for public release; distribution is unlimited

THIS PAGE INTENTIONALLY LEFT BLANK

REPORT DOCUMENTATION PAGE			Form Approved OMB No. 0704-0188
Public reporting burden for this collection of information is estimated to average 1 hour per response, including the time for reviewing instruction, searching existing data sources, gathering and maintaining the data needed, and completing and reviewing the collection of information. Send comments regarding this burden estimate or any other aspect of this collection of information, including suggestions for reducing this burden, to Washington headquarters Services, Directorate for Information Operations and Reports, 1215 Jefferson Davis Highway, Suite 1204, Arlington, VA 22202-4302, and to the Office of Management and Budget, Paperwork Reduction Project (0704-0188) Washington DC 20503.			
1. AGENCY USE ONLY ***(Leave blank)***	**2. REPORT DATE** September 2007	**3. REPORT TYPE AND DATES COVERED** Master's Thesis	
4. TITLE AND SUBTITLE Maritime Surveillance Using a Wideband Hydrophone			**5. FUNDING NUMBERS**
6. AUTHOR(S) Jason Keith Wilson			
7. PERFORMING ORGANIZATION NAME(S) AND ADDRESS(ES) Naval Postgraduate School Monterey, CA 93943-5000			**8. PERFORMING ORGANIZATION REPORT NUMBER**
9. SPONSORING /MONITORING AGENCY NAME(S) AND ADDRESS(ES) SPAWAR Systems Center San Diego, CA 92152 Office of Naval Research Arlington, VA 22203			**10. SPONSORING/MONITORING AGENCY REPORT NUMBER**
11. SUPPLEMENTARY NOTES The views expressed in this thesis are those of the author and do not reflect the official policy or position of the Department of Defense or the U.S. Government.			
12a. DISTRIBUTION / AVAILABILITY STATEMENT Approved for public release; distribution is unlimited			**12b. DISTRIBUTION CODE**

13. ABSTRACT (maximum 200 words)

Undersea acoustic modems acquire wideband acoustic time series through an electro-acoustic transducer and use on-board digital signal processing for receiving acoustic communications. These component devices can potentially serve a dual use for passive sensing of radiated acoustic energy from maritime vessels. This thesis examines the characteristic Lloyd's mirror interference pattern present in the acoustic spectrogram of a passing surface target and applies two-path ray theory and waveguide invariant theory to an analysis of the phenomenon. The two theories are shown to be mathematically equivalent under certain conditions. In combination with the Doppler shift from a target tonal, these theories permit a calculation of target range and speed at the closest point of approach (CPA). Such analysis is applied to spectrograms obtained in a controlled experiment at the approaches to San Diego Bay. For targets passing within 185 meters of the receiver, the resulting Lloyd's mirror pattern permits calculation of the range to within 9%. Target speed obtained from the Doppler shift is within 4% of the ground truth value.

14. SUBJECT TERMS undersea warfare, acoustic modem, shallow water acoustic detection, Doppler shift, Lloyd's mirror, ray theory, waveguide invariant, multipath propagation, underwater acoustics, maritime surveillance			**15. NUMBER OF PAGES** 69
			16. PRICE CODE
17. SECURITY CLASSIFICATION OF REPORT Unclassified	**18. SECURITY CLASSIFICATION OF THIS PAGE** Unclassified	**19. SECURITY CLASSIFICATION OF ABSTRACT** Unclassified	**20. LIMITATION OF ABSTRACT** UU

NSN 7540-01-280-5500

Standard Form 298 (Rev. 2-89)
Prescribed by ANSI Std. 239-18

THIS PAGE INTENTIONALLY LEFT BLANK

Approved for public release; distribution is unlimited

MARITIME SURVEILLANCE USING A WIDEBAND HYDROPHONE

Jason K. Wilson
Lieutenant, United States Navy
B.S., University of Missouri, Columbia, 2000

Submitted in partial fulfillment of the
requirements for the degree of

MASTER OF SCIENCE IN ENGINEERING ACOUSTICS

from the

NAVAL POSTGRADUATE SCHOOL
September 2007

Author: Jason K. Wilson

Approved by: Joseph A. Rice
Thesis Advisor

Daphne Kapolka
Co-Advisor

Paul Hursky
Co-Advisor

Kevin B. Smith
Chair, Engineering Acoustics Academic Committee

THIS PAGE INTENTIONALLY LEFT BLANK

ABSTRACT

Undersea acoustic modems acquire wideband acoustic time series through an electro-acoustic transducer and use on-board digital signal processing for receiving acoustic communications. These component devices can potentially serve a dual use for passive sensing of radiated acoustic energy from maritime vessels. This thesis examines the characteristic Lloyd's mirror interference pattern present in the acoustic spectrogram of a passing surface target and applies two-path ray theory and waveguide invariant theory to an analysis of the phenomenon. The two theories are shown to be mathematically equivalent under certain conditions. In combination with the Doppler shift from a target tonal, these theories permit a calculation of target range and speed at the closest point of approach (CPA). Such analysis is applied to spectrograms obtained in a controlled experiment at the approaches to San Diego Bay. For targets passing within 185 meters of the receiver, the resulting Lloyd's mirror pattern permits calculation of the range to within 9%. Target speed obtained from the Doppler shift is within 4% of the ground truth value.

THIS PAGE INTENTIONALLY LEFT BLANK

TABLE OF CONTENTS

THIS PAGE INTENTIONALLY LEFT BLANK

LIST OF FIGURES

THIS PAGE INTENTIONALLY LEFT BLANK

LIST OF TABLES

THIS PAGE INTENTIONALLY LEFT BLANK

ACKNOWLEDGEMENTS

I would like to thank the following people for their support:

First and foremost to my wife and best friend Amy, for her love, patience and encouragement and for giving me two wonderful daughters, Arwen and Ayden.

To my mother Wanda, for instilling in me discipline and a hard work ethic, two prerequisites for the successful navigation of a master's program.

To my thesis advisor and mentor Joe Rice, who initially sparked my interest in underwater communications and surveillance and set the conditions to make my research an outstanding success.

To my co-advisor Professor Daphne Kapolka, for her assistance and support throughout my time at NPS.

To Paul Hursky for his assistance at Zuniga `07 and throughout the thesis process.

To Doug Grimmett, Robert Creber, and Lonnie Hamme from SPAWAR Systems Center San Diego, for their support during Zuniga `07.

Finally, to my father Larry, in whose memory I dedicate this thesis.

THIS PAGE INTENTIONALLY LEFT BLANK

I. INTRODUCTION

A. BACKGROUND

Acoustic modems are emerging as a routine means for communication with undersea autonomous sensors and instruments. As networks of acoustic modems become pervasive in the undersea environment, the opportunity arises to use the modems themselves for sensing the acoustic field and detecting the presence of maritime vessels. Radiated noise from target vessels includes characteristic features of propulsion, cavitation, machinery, fathometer, obstacle avoidance sonar, etc.

With acoustic spectrograms obtained from a controlled experiment, this thesis uses Doppler shift, two-path ray theory, and the waveguide invariant method to estimate range and speed as a target passes through closest point of approach (CPA). Whereas two-path ray theory is expected to work at relatively short ranges, the waveguide invariant method is expected to work at longer ranges where a normal-mode description of the acoustic field is valid.

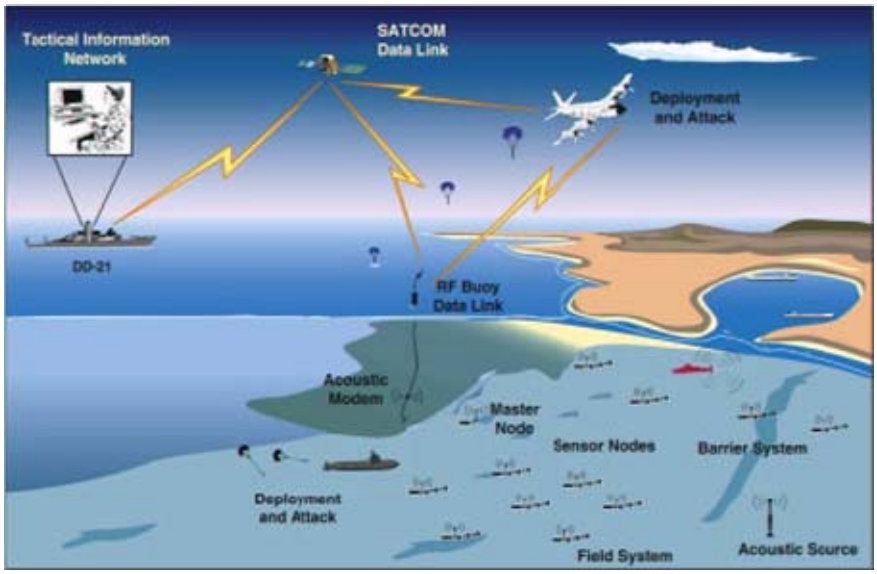

Figure 1. Deployable Autonomous Distributed System [From Tom Roy, SPAWAR Systems Center San Diego].

B. RESEARCH MOTIVATION

Through its ability to detect, track, and identify targets of interest, an undersea sensing network employing acoustic modems for detection and communication could greatly enhance both domestic port security and international maritime surveillance. Figure 1 depicts this concept for a developmental undersea warfare (USW) application.

The goal of this thesis is to develop a capability for passively sensing the passage of ships and submarines by processing acoustic time series incidentally obtained by an undersea acoustic modem. Once developed, the ability of an underwater acoustic modem to act as a passive sensor has many tactical applications. One possible scenario includes clandestinely seeding a channel or harbor where a chokepoint exists for inbound or outbound shipping. This underwater "picket line" could report contacts of interest directly to manned control centers or provide cuing to national sensors. Future technological improvements could include acoustic fingerprinting where the sensors only report on certain designated types of targets. Figure 2 depicts a representative target, its associated acoustic time series, and acoustic spectrogram. The spectrogram shows the characteristic Lloyd's mirror interference pattern typical of a target traveling past the hydrophone. The objective here is to use these data to estimate the target speed and range at CPA.

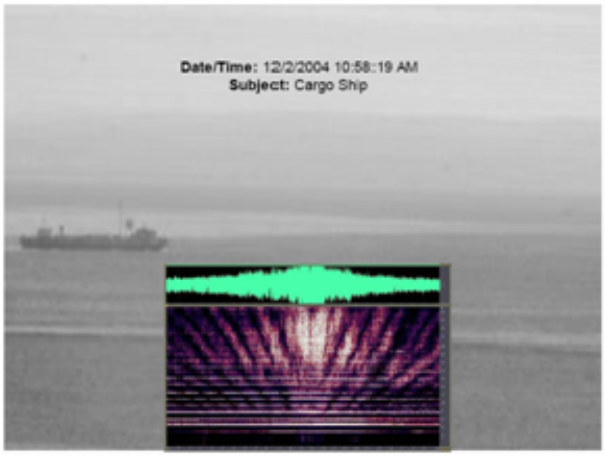

Figure 2. A surface ship, associated acoustic time series and acoustic spectrogram as detected by a single fixed hydrophone [From Brian Granger, SPAWAR Systems Center].

C. SUMMARY OF THESIS

This thesis is limited to the estimation of speed and range of a surface contact from spectrograms which contain narrowband tonals from a target passing through CPA and a Lloyd's mirror interference pattern in the broadband component.

The theoretical framework for the two-path ray theory method and the waveguide invariant method is developed. Strengths and limitations of each method are presented in relation to how they apply to the operational scenario.

The data sets analyzed in this research were obtained from a controlled experiment in San Diego Bay. The Zuniga `07 experiment recorded the acoustic signatures produced by a small surface craft as it traveled along prescribed paths at various ranges and speeds. Several of these data sets have discernable Lloyd's mirror patterns and Doppler shifts as the target passes through CPA.

The two-path ray theory method is applied to the usable data sets to estimate the range of the boat. Results are then compared to ground-truth GPS (Global Positioning System) navigation to determine the validity of the approach. It is shown how the utility of each method deteriorates as the CPA range increases and the striations in the Lloyd's mirror image become less apparent. Finally, recommendations for future work to further develop the passive sensing capability of underwater acoustic modems are presented.

THIS PAGE INTENTIONALLY LEFT BLANK

II. THEORY

A. TWO-PATH RAY THEORY

Sound in the ocean can propagate from a source to a receiver via multiple paths. This thesis specifically considers sound reaching a receiver via a direct (non-reflected) path and via a surface reflected path. If the sea surface boundary is sufficiently smooth, the sound energy may reach the receiver through surface reflection and interfere with the direct path arrival. [Urick, 1983] states that:

> If the sea surface were perfectly smooth, it would form an almost perfect reflector of sound. The intensity of sound reflected from the smooth sea surface would be very nearly equal to that incident upon it. When the sea surface is not too rough, it creates an interference pattern in the underwater sound field. This pattern is caused by constructive and destructive interference between the direct and surface reflected sound and is called the Lloyd's mirror, or image interference effect.

The reason why the surface needs to be fairly smooth to get an interference pattern lies in the requirement that the sound reaching the receiver along different paths be coherent, i.e. that the paths have constant phase difference between them. If the sound received from different paths is incoherent, the received intensity is the sum of the intensity coming from each separate path and the deep nulls which characterize interference are absent. The depth of the nulls also depends on the amplitude of the sound coming along the different paths. To the extent that the sound from two coherent paths is of equal amplitude, the pressure at the nulls will be zero. In general, this requirement is met most frequently at short ranges when wave action and turbulence are minimal. It is also more likely to be met by surface reflections due to the fact that virtually 100% of the sound energy is reflected off a water-air interface thus making the amplitude of the direct and reflected path of approximately equal amplitude. The same interference effect can apply to bottom bounce propagation too; however, bottom type strongly influences the amount of energy reflected or refracted back into the water column. Rocky or sandy bottoms reflect sound energy more strongly than soft mud or

silt. The following section presents a mathematical explanation of the cause of the Lloyd's mirror pattern seen in spectrograms and presents a means of determining target range and speed at CPA based on the Lloyd's mirror pattern and the Doppler shift of narrowband tonals. The analysis in this work assumes that the target maintains a constant course and speed as it passes through CPA. Since Lloyd's mirror patterns are frequently seen at fairly short ranges due to the interference between a surface reflected and direct path, refraction is ignored in the following discussion. In most cases this should be a reasonable approximation. Even with pronounced sound speed gradients the radius of curvature of the sound rays tends to be quite large. However, the method could certainly be extended to include refraction if required. It should also be pointed out that at long ranges, many more multi-path interactions which would need to be considered. For this reason, ray theory would be difficult to apply.

1. Geometric Explanation of Surface Interference

Figure 3 provides a diagram of the basic geometry for analyzing surface interference on the basis of simple straight-line propagation for both a direct and surface reflected path. If the surface is smooth enough, sound energy incident on the surface will reflect back at an angle equal to the angle of incidence. The source, B, is *d* meters below the surface and radiating both broadband and narrowband noise. The receiver, D, is *h* meters below the surface. Sound energy emanating from the source can either follow a direct path to the receiver, annotated by r_d, or a surface reflected path, r_s. The horizontal distance between the source and the receiver is denoted by *r*.

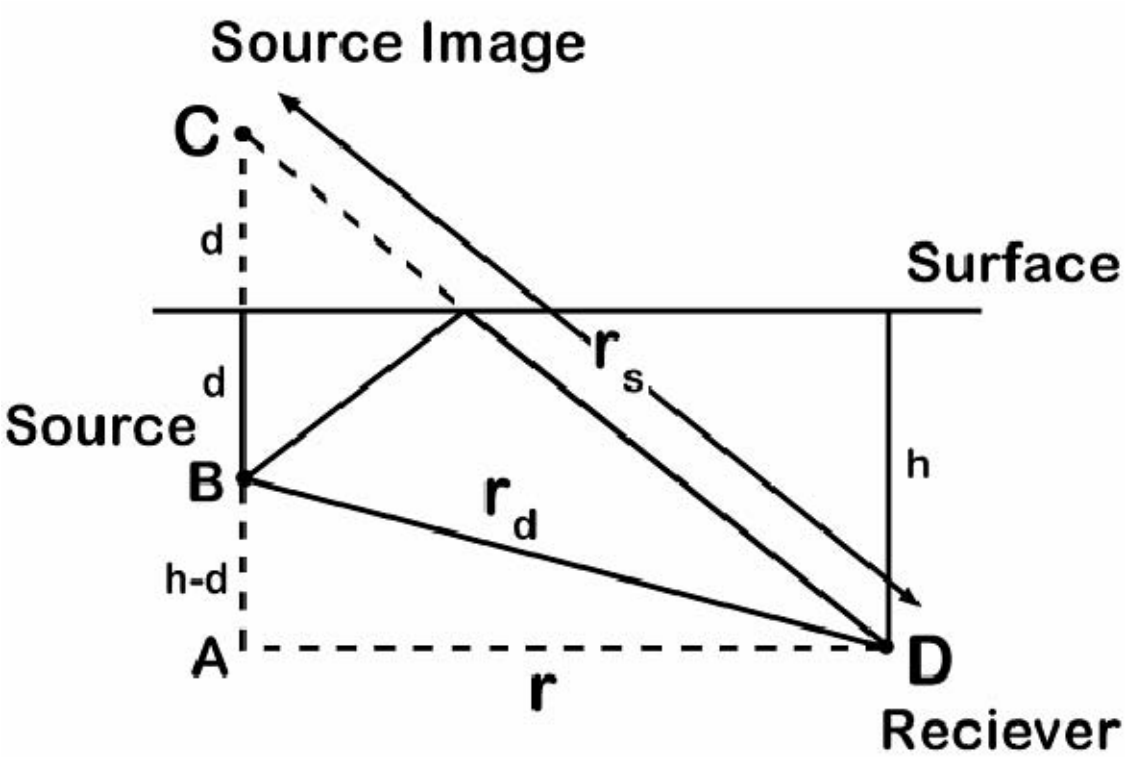

Figure 3. Geometry for analyzing surface interference [From Kapolka, 2007].

It is clear from the picture that r_s and r_d are unequal, with $r_s > r_d$. This difference in path length can result in an interference pattern if the sound propagating along the two paths is coherent. Assuming that $r>>h+d$, the path-length difference is approximately equal to

$$\Delta r = \frac{2hd}{r}. \tag{2.1}$$

Because of the 180^o phase shift which occurs upon surface reflection, pressure minima, or nulls, occur where the path length difference between the direct and reflected paths is equal to an integral number of wavelengths. This gives the ranges to the nulls as

$$r_n = \frac{2hd}{n\lambda} = \frac{2hd}{nc} f. \tag{2.2}$$

Rearranging this expression yields the nulled frequencies as a function of range

$$f_n = \frac{nc}{2hd} r \,. \tag{2.3}$$

These equations give the ranges at which certain frequencies will be nulled, or, conversely, which frequencies can be expected to be nulled as a function of range. In either case, this means that as the range between source and receiver changes, the frequencies which have nulls at the receiver also change. This treatment is generally considered to be valid for fairly short ranges where the decorrelating effects of ocean turbulence, wave action, and multipath structure have not destroyed the observed coherence of the direct and surface reflected paths.

2. Lloyd's Mirror

A broadband spectrogram is shown in Figure 4. The light (unshaded) hyperbolic shaped regions, commonly called "striations" centered about $t = 0$ are the nulls from the Lloyd's mirror interference pattern for the broadband noise. The frequency values F_1, F_2 etc. represent the minimum frequency, F_n of each hyperbola. The actual frequency from the sound source that is being nulled by the surface reflection varies with time as the hyperbolas are traced out. These families of hyperbolae are often described as a "bathtub" pattern appearing in the spectrogram.

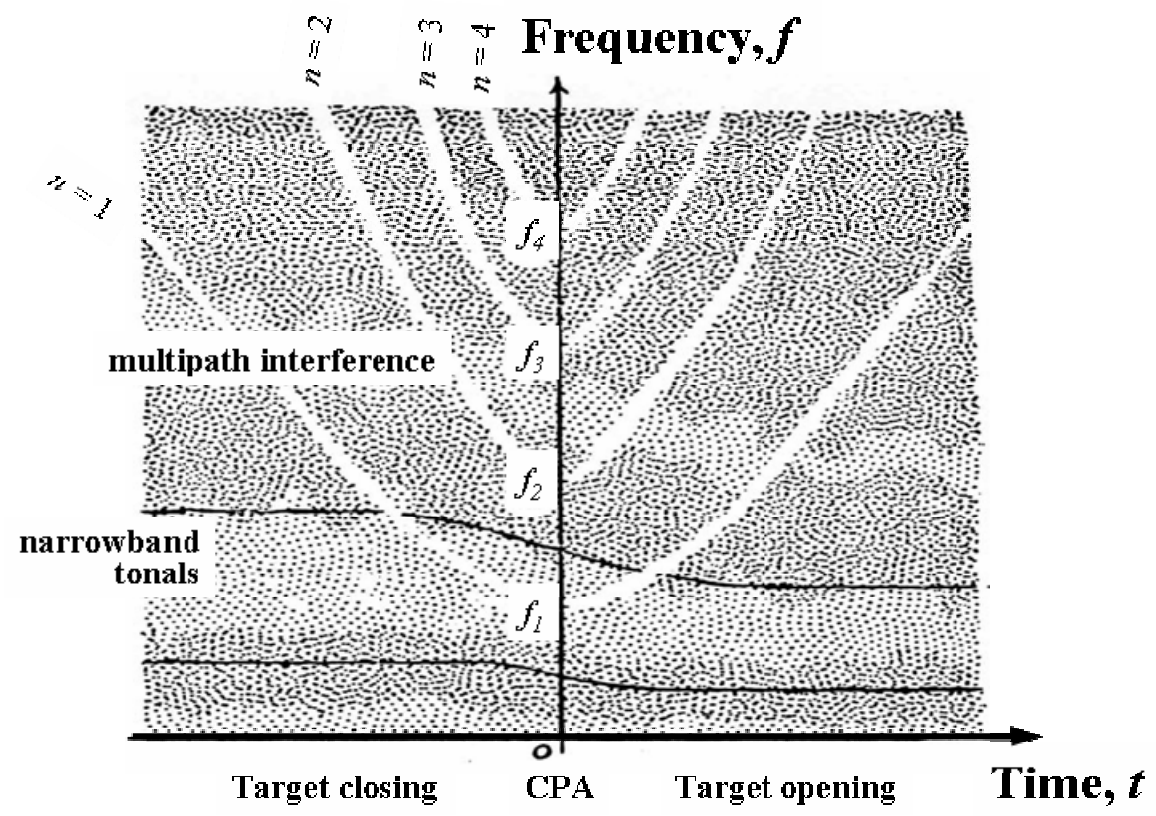

Figure 4. Frequency vs. time display of Lloyd's mirror interference pattern [After Hudson, 1987].

An analysis of the geometry shown in Figure 5 explains why the striations have the shape of hyperbolae in the spectrogram. In this figure, a target is traveling along a constant course with a speed of *v*. If $t = 0$ is taken as the time of CPA, the range to CPA is given by *vt*. The instantaneous range of the target to the receiver is given by *r*, and range at CPA is R_o.

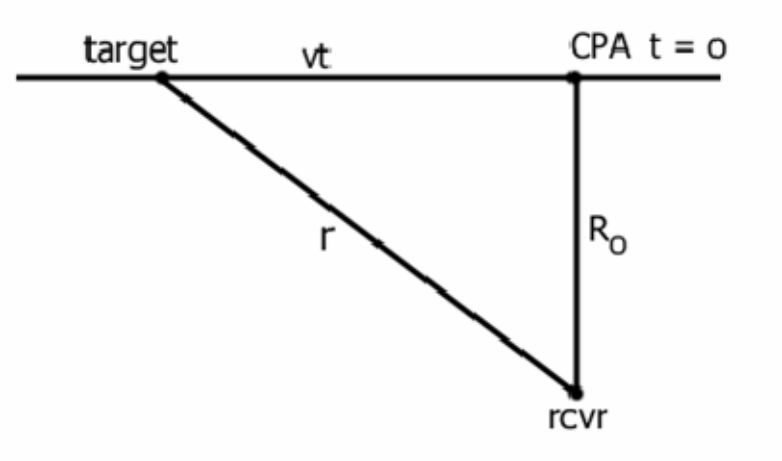

Figure 5. Geometry for analyzing a spectrogram pattern for a target passing through CPA [From Kapolka, 2007].

By the Pythagorean Theorem, the distance to the target at any time, *t*, is given by

$$r = \sqrt{R_o^{\,2} + vt^2}\,. \tag{2.4}$$

Substituting the expression for the frequencies which are nulled as a function of the range, (2.3), into this expression and rearranging yields

$$R_o^{\,2} = \left(\frac{2hd}{nc}\right)^2 f_n^{\,2} - v^2 t^2\,. \tag{2.5}$$

This shows that the nulled frequencies trace out the pattern of nested hyperbolae with respect to time.

3. Measuring Speed and Range at CPA

The combination of the hyperbolic Lloyd's mirror pattern produced by the emission of broadband energy from a target and the target's discrete tonals can be exploited to produce a tracking solution. If a target has an observable tonal its frequency undergoes an apparent frequency change, or Doppler shift, as the target closes range, passes CPA and then opens range. Doppler shift of narrowband tonals is depicted in Figure 4. The center frequency, f_o, can be calculated as

$$f_o = \frac{f_u + f_l}{2} \ , \tag{2.6}$$

where f_u is the maximum closing frequency and f_l is the minimum opening frequency. The target tonal approaches this maximum and minimum frequency asymptotically as the target range becomes large relative to the CPA range, because the component of velocity along the line of sound approaches the target velocity. The maximum Doppler shift is then given by

$$\Delta f = f_u - f_o = f_o \frac{v}{c} . \tag{2.7}$$

Rearranging for the velocity, v, gives

$$v = c \frac{\Delta f}{f_o} . \tag{2.8}$$

Therefore, if the target has a discernable tonal as it passes through CPA, its velocity can be estimated from the Doppler shift.

By examining the hyperbolic Lloyd's mirror pattern of the target, an estimate of the target range at CPA can also be developed. First, a determination of how the frequency of the sound is changing in time as the target approaches CPA must be recovered. This is determined by measuring the slope of a regression line plotted along a striation. Taking the derivative of (2.3) with respect to time and equating $dr/dt = v$, the slope along a striation is given by

$$\frac{df_n}{dt} = \frac{ncv}{2hd} . \tag{2.9}$$

It is important to measure the slope of the striation line at long ranges where the slope is linear as it approaches its asymptotic value. Not only does this validate the assumption that $dr/dt = v$, but it also decreases the uncertainty by providing more points in the slope calculation.

Returning to (2.5), it is evident that the range r is given by

$$r = \frac{2hd}{nc} f_n . \tag{2.10}$$

Substituting (2.9) into (2.10) produces

$$r = \frac{vf_n}{df_n / dt} . \tag{2.11}$$

This expression is valid at ranges which are long compared to the CPA range since it depends on the assumption that all the target velocity is along the line of sound. Finally, by using the value of the target range, r, the velocity as determined by the Doppler shift, and the time over which the measurement was made, the target range at CPA can be determined from (2.4) as

$$R_o = \sqrt{\left(\frac{vf_n}{df_n / dt} \right)^2 - (vt)^2} . \tag{2.12}$$

If instead of differentiating (2.3) with respect to time it is differentiated with respect to distance, it yields

$$\frac{df_n}{dr} = \frac{nc}{2hd} . \tag{2.13}$$

Substituting $\frac{nc}{2hd} = \frac{f_n}{r}$ from (2.10) into this expression yields the more general result

$$\frac{df_n}{dr} = \frac{f_n}{r} \tag{2.14}$$

This expression is valid at any range as long as the assumption $r >> h+d$ holds. It is also interesting to note that (2.10) predicts that the ratio of nulled frequency to range should be a constant for each striation, i.e.,

$$\frac{nc}{2hd} = \frac{f_n}{r} = \text{constant} . \tag{2.15}$$

B. THE WAVEGUIDE INVARIANT

1. Background

Originally introduced by the Russian scientists Chuprov, Grachev, Brekhovskikh and Lysanov, the waveguide invariant method provides an alternative model for the striations in "bathtub" patterns observed when sources pass through CPA. Following the earlier Russian work, D'Spain and Kuperman describe how the striations can also arise from the interference between normal modes, thus explaining why such interference patterns occur well beyond the ranges at which the two-path Lloyd's mirror model is valid. The waveguide invariant theory provides a convenient framework for the analysis of these interference patterns. This theory shows how a single scalar parameter β, called the acoustic invariant, summarizes the dispersive characteristics of the acoustic field in a waveguide [D'Spain and Kuperman, 1999].

2. The Waveguide Invariant

The original equation for β, as defined by Brekhovskikh and Lysanov, is

$$\beta = \frac{r}{\omega}\frac{d\omega}{dr} = -\frac{d\left(1/v\right)}{d\left(1/u\right)}\ , \tag{2.16}$$

where r is the range along the line of sight from source to receiver and $d\omega/dr$ is the derivative or slope of the angular frequency with respect to range at which the striation nulls occur [Brekhovskikh et. al., 2003]. The quantities $d\left(1/v\right)$ and $d\left(1/u\right)$ are the derivatives of the phase slowness and group slowness respectfully. The phase slowness and group slowness are simply the inverses of the phase and group velocities for that particular mode.

When the range between the source and receiver is much greater than the range at CPA, all of the motion is along the line of propagation. Therefore, $\delta\omega/\delta r$ may be expressed as $\delta\omega/v\delta t$. Putting (2.16) in terms of $\delta\omega/\delta t$ and velocity, *v*, yields

$$\frac{d\omega}{dt} = \beta\omega\frac{v}{r}. \tag{2.17}$$

This equation can be expressed in terms of frequency instead of angular frequency and rearranged to yield

$$r = \frac{\beta v f}{df\,/\,dt}\,. \tag{2.18}$$

Since the angular frequency in the above equations refers to the frequency at which striation nulls occur, this expression is identical to the two-path ray theory result presented in (2.11) as long as β is equal to one.

Rearranging Brekhovskikh and Lysanov's expression in (2.16) and integrating in an environment where β is constant yields

$$\int \frac{d\omega}{\omega} = \beta \int \frac{dr}{r} \quad \text{or} \quad \ln \frac{\omega(t)}{\omega_o} = \beta \ln \frac{r(t)}{r_o}\,, \tag{2.19}$$

where ω_o and r_o are the nulled angular frequency and range at some arbitrary point in time along a striation.

Kuperman and D'Spain exponentiate this term to express it in their 2001 paper as

$$\omega(t) = \omega_o \left(\frac{r(t)}{r_o} \right)^{\beta}. \tag{2.10}$$

Again it should be noted that for $\beta = 1$, this result is identical to the result of the two-path ray theory method since it predicts that the ratio of the nulled frequency to the range should be a constant.

Problems arise when β varies with range or azimuth. In these cases, beta can be calculated if we know something about the bathymetry and other parameters of the ocean waveguide at the locations of the source and receiver. This is obviously problematic if the goal is to discover the source range. Fortunately, as long as sound energy does not refract significantly into the bottom and the bottom depth is constant, β does not often deviate very much from one [D' Spain and Kuperman, 1999].

Recent work by Lee and Makris in their 2006 paper suggests a novel approach to the problem of source range estimation using the output of an array beamformer. They

call this the “array invariant” method. This approach was not pursued for this thesis since it requires an extended aperture of multiple sensors.

THIS PAGE INTENTIONALLY LEFT BLANK

III. EXPERIMENT

A. ZUNIGA `07 OVERVIEW

Zuniga `07 was an experiment conducted in San Diego Bay on the 30th of July 2007 with support from SPAWAR Systems Center, San Diego. The objective of Zuniga `07 was to obtain acoustic data sets of a source target traveling along known tracks at known speeds in an operationally representative environment.

The test plan called for multiple passes by a small boat at known range and speed past a moored sonobuoy. The hydrophone was one meter above the seabed and was connected to a floating buoy housing a VHF transmitter. The sensed acoustic energy was transmitted back to the shore station for recording and analysis. Figure 6 shows the intended tracks and location of the sonobuoy in San Diego Bay. Table 1 lists the prescribed tracks and intended CPA distances to the sonobuoy.

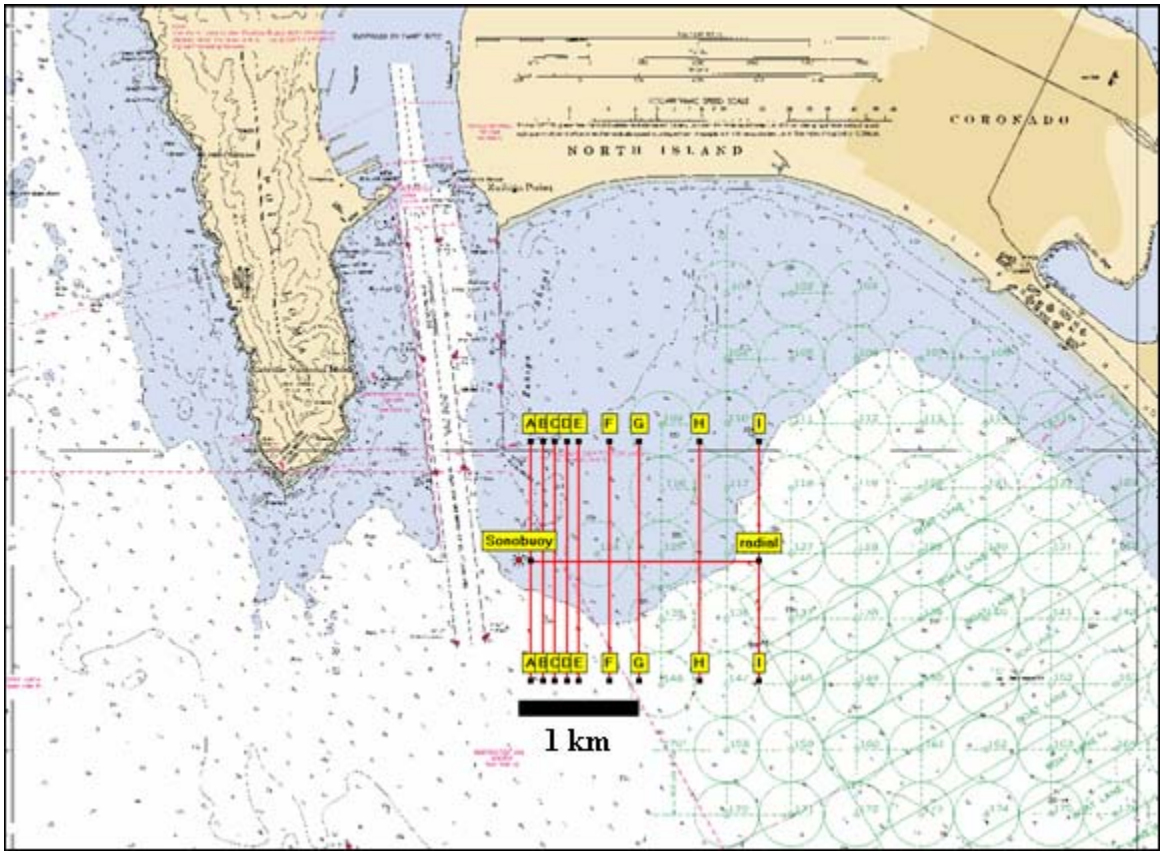

Figure 6. Zuniga `07 proposed tracks.

Track	Endpoint	Endpoint	Endpoints	Heading	CPA to Sonobuoy (meters)	Speed (knots)
A	32° 40.04′ N	32° 38.96′ N	117° 13.2359′ W	0 or 180 T	100	15
B	32° 40.04′ N	32° 38.96′ N	117° 13.1717′ W	0 or 180 T	200	15
C	32° 40.04′ N	32° 38.96′ N	117° 13.1076′ W	0 or 180 T	300	15
D	32° 40.04′ N	32° 38.96′ N	117° 13.0435′ W	0 or 180 T	400	15
E	32° 40.04′ N	32° 38.96′ N	117° 12.9793′ W	0 or 180 T	500	15
F	32° 40.04′ N	32° 38.96′ N	117° 12.8190′ W	0 or 180 T	750	15
G	32° 40.04′ N	32° 38.96′ N	117° 12.6586′ W	0 or 180 T	1000	15
H	32° 40.04′ N	32° 38.96′ N	117° 12.3380′ W	0 or 180 T	1500	15
I	32° 40.04′ N	32° 38.96′ N	117° 12.0173′ W	0 or 180 T	2000	15
R	117° 13.235′W	117° 12.017′W	32° 39.50′ N	270 T	<100	15
J	32° 40.04′ N	32° 38.96′ N	117° 12.3380′ W	0 or 180 T	1500	7
K	32° 40.04′ N	32° 38.96′ N	117° 12.0173′ W	0 or 180 T	2000	7

Table 1. Zuniga `07 target track plan.

B. ENVIRONMENTALS AND BACKGROUND SHIPPING

Winds on the test day were north-northwest at 8-10 miles per hour. Seas were 2-4 feet trough-to-crest with approximately a 5-second period. Bottom type throughout the operating area is sand. Figure 7 is a graph of the sound-speed profile derived from a CTD cast conducted on 1 July, one day after the acoustic events.

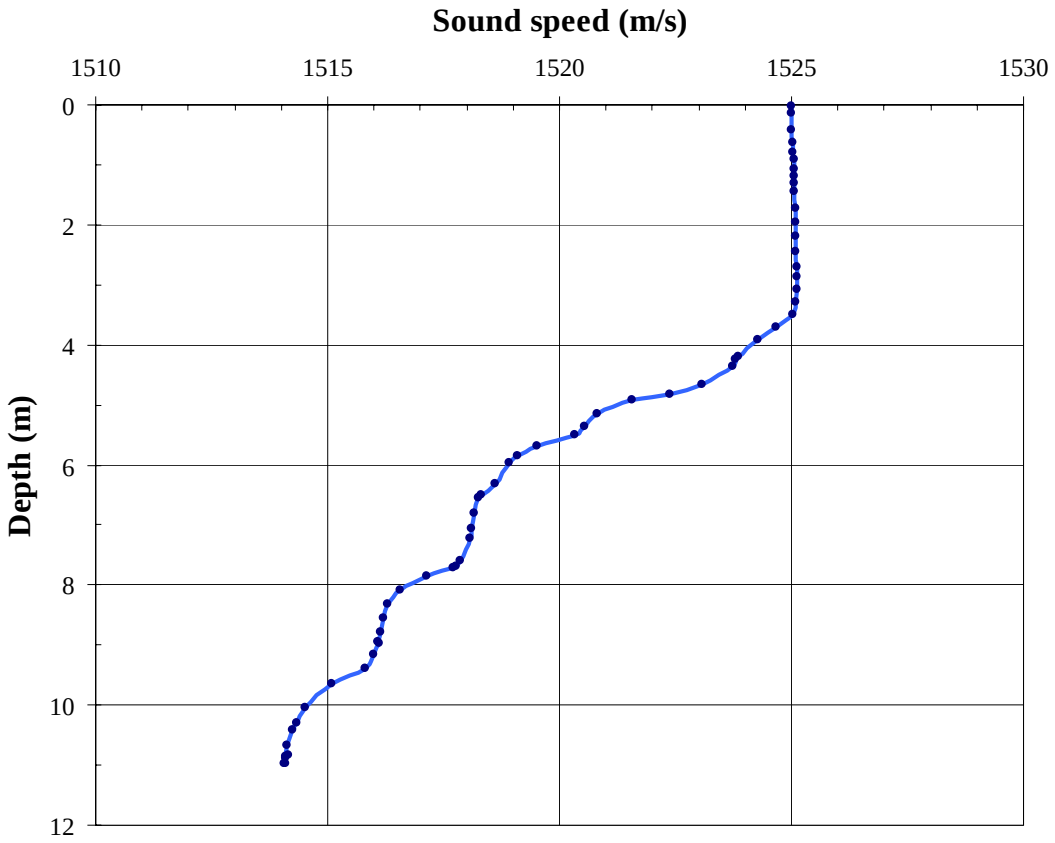

Figure 7. Sound-Speed Profile, San Diego Harbor August 1, 2007.

The conduct of the test on a Monday yielded mostly pleasure craft, although at times, local traffic was heavy. Throughout the afternoon, most of the pleasure craft in the area stayed on the opposite side of the shipping channel. No motorized surface craft were logged within 500 meters of the target boat. Recording was suspended whenever a naval vessel was in the immediate area.

C. SETUP

The shore recording station was located on the 4th floor of the Bachelor Officers Quarters (BOQ) at Naval Submarine Base, Point Loma. This position offered a clear line of sight to the operations area. The analog sonobuoy signal was relayed via VHF channel 32 to a receiver antenna mounted on the balcony of the BOQ room. Communications between this shore station and the source boat were via VHF handheld radios and/or cell phone.

Figure 8. Zuniga `07 operations area.

The target boat used for the test was a 24-ft Navy Harbor Security Boat owned and operated by SPAWAR Systems Center, San Diego. This V-hulled boat, shown in Figure 9, is diesel-powered with outboard engines, dual propellers, and exhaust through the propeller hub.

Figure 9. 24-ft Navy harbor security craft.

The sonobuoy used for Zuniga `07 was procured from SeaLandAire Technologies. It consists of a modified sonobuoy radio transmitter antenna mounted to a rigid foam float, as seen in Figure 10. The float holds modules that contain rechargeable batteries, electronics and VHF antenna for signal transmission to the shore station. The hydrophone, shown in Figure 11, was anchored 1 meter off the bottom at a depth of approximately 9 meters and electrically tethered to the floating communications buoy.

Figure 10. SeaLandAire floating communications buoy.

Figure 11. SeaLandAire hydrophone.

Two GPS data recording devices, such as that seen in Figure 12, were used during the experiment. One was placed on the floating communications buoy to account for any displacement of the anchor during the experiment. This was necessary because a prior experiment suffered from tampering and relocation of the sonobuoy by a boater. Another was mounted on the target boat to record a continuous log of position. Logged data include latitude, longitude, course, speed, and time with sampling at 1-2 second intervals. Upon completion of the test, the recorded position data from each GPS logger were downloaded to a computer file.

Figure 12. Ohararp GPS data logger.

D. GROUND TRUTH

There is a substantial difference between the intended tracks as prescribed by the test plan and the actual tracks. This is attributed to the roughness of the sea during the afternoon and the handling characteristics of the boat. The priority during the test was to ensure constant course and speed over the track. The desired CPA distances were not as critical, since the actual CPA ranges are readily calculated from the GPS data.

Table 2 provides a description of the actual CPA ranges and speeds of the target boat during the experiment. Velocity is computed by taking the distance traveled by the boat over the track divided by the total time of the track.

TRACK	A	B	C	D	E	F	G	H	I	R	J	K
CPA (m)	54	97	185	241	396	576	830	1384	1824	74	97	148
Velocity (m/s)	5.6	5.8	5.9	6.4	6.4	6.0	5.3	6.0	5.3	5.9	3.4	3.4

Table 2. Ground-truth CPA and velocity of target boat.

The following figures show the actual target tracks as recorded by the onboard GPS logger. Velocity and COA annotations are based on the GPS logger data.

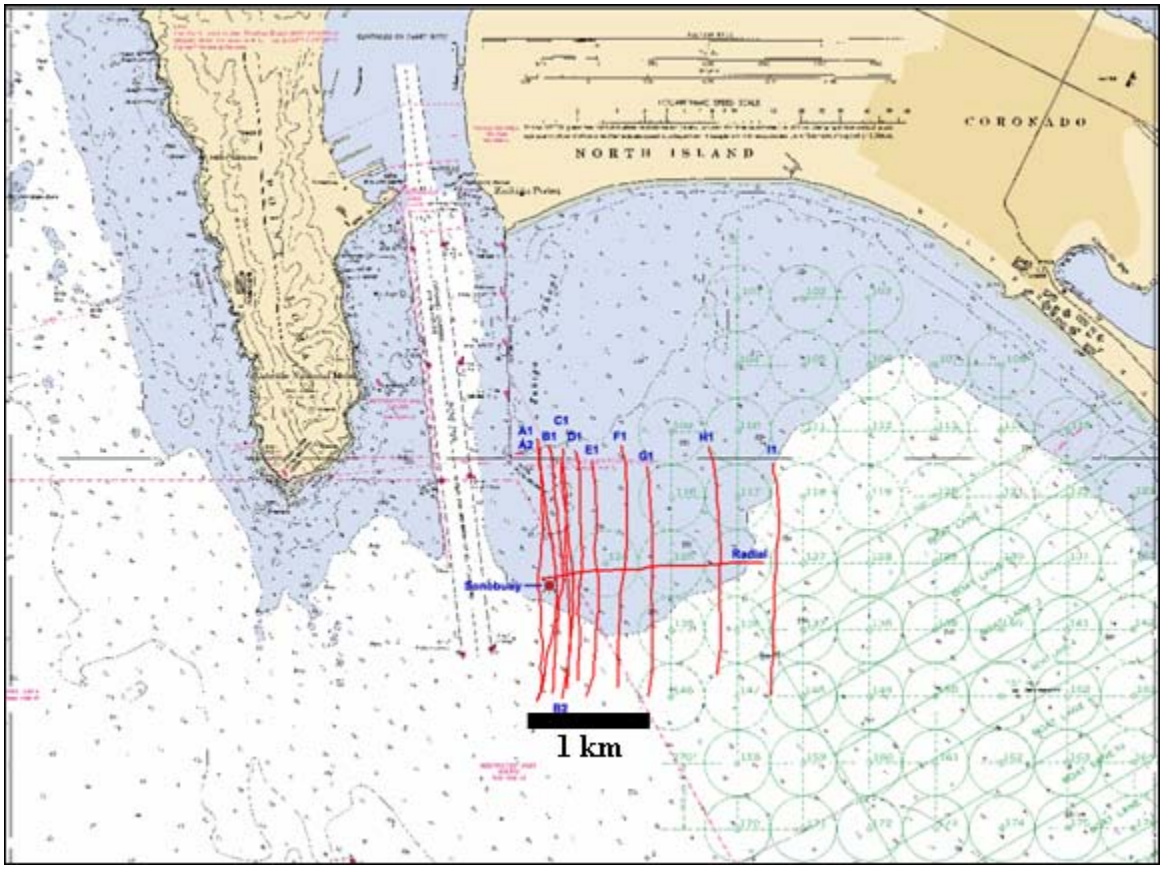

Figure 13. Zuniga `07 all tracks.

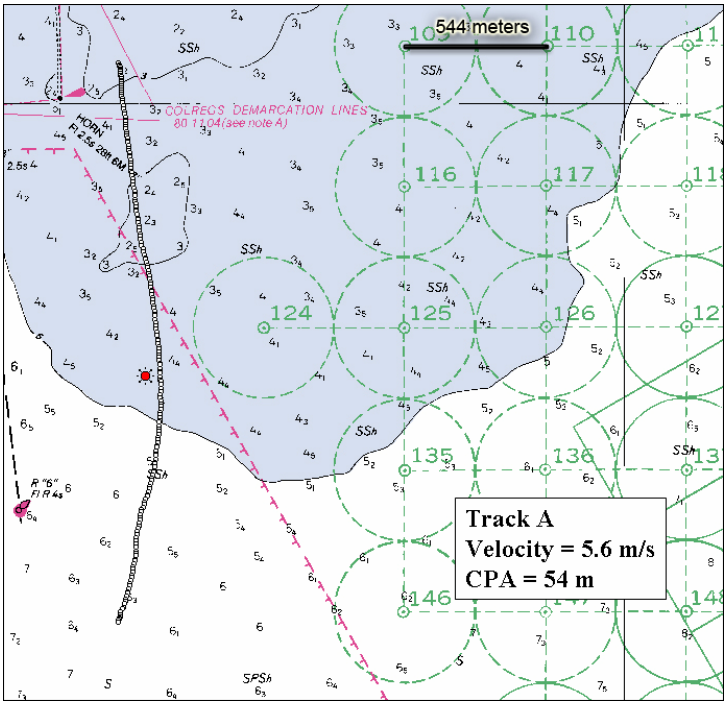

Figure 14. Track A.

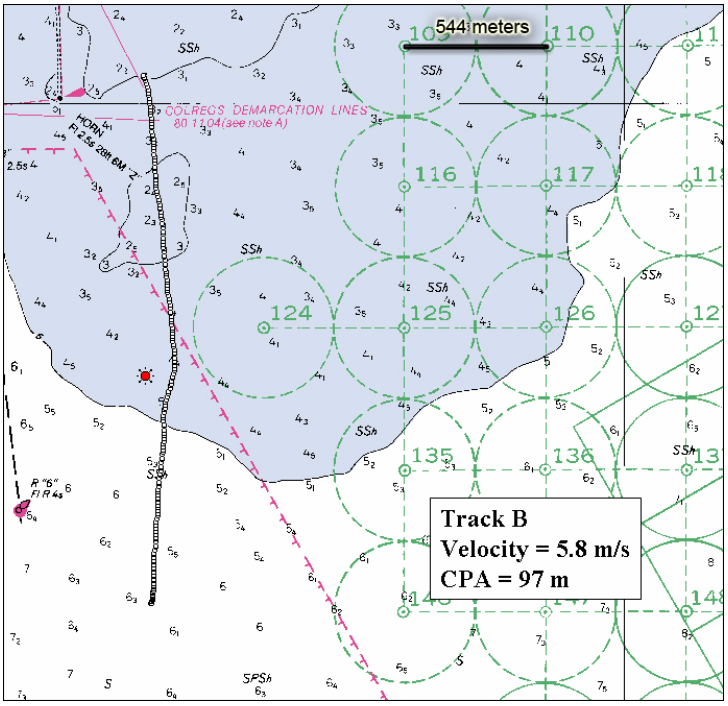

Figure 15. Track B.

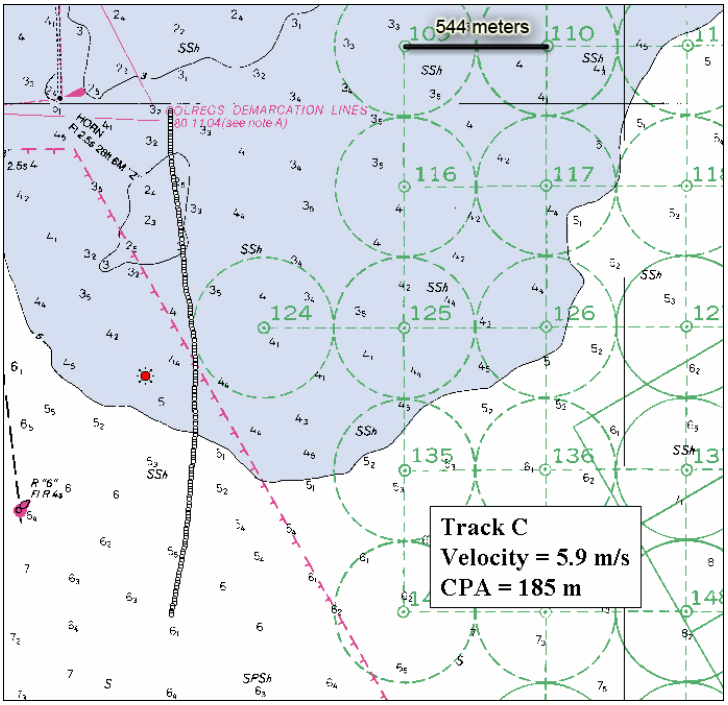

Figure 16. Track C.

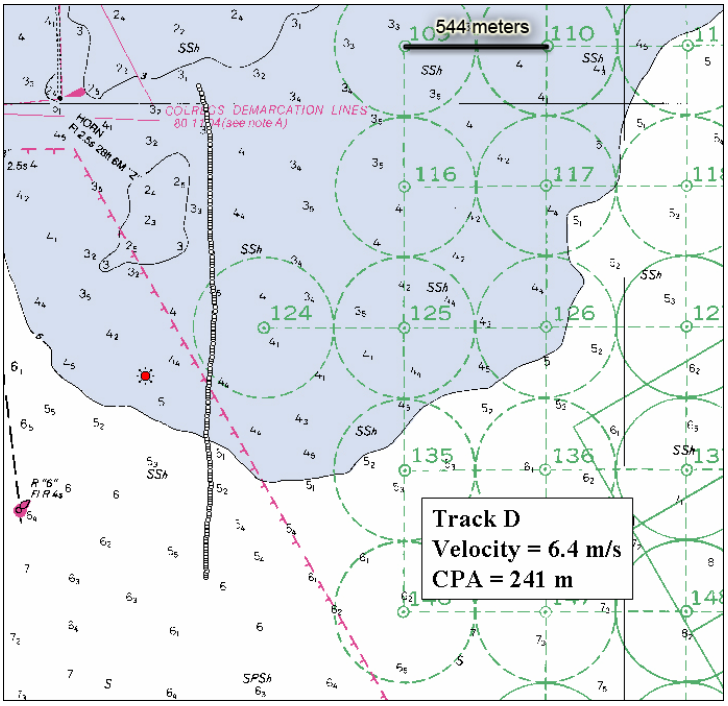

Figure 17. Track D.

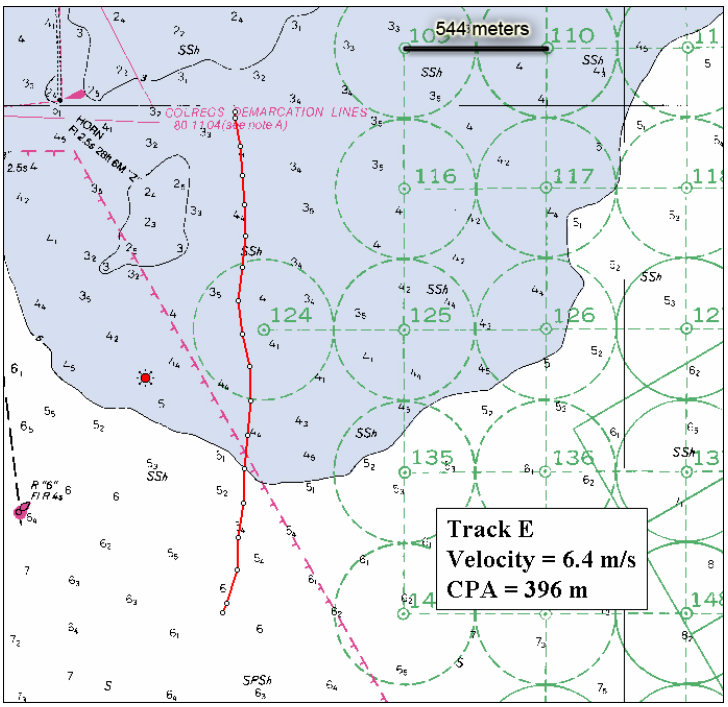

Figure 18. Track E.

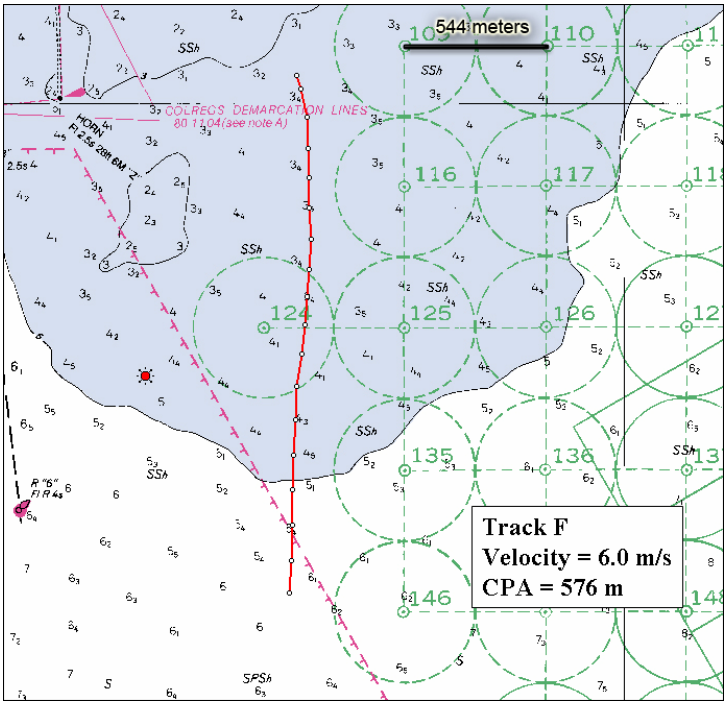

Figure 19. Track F.

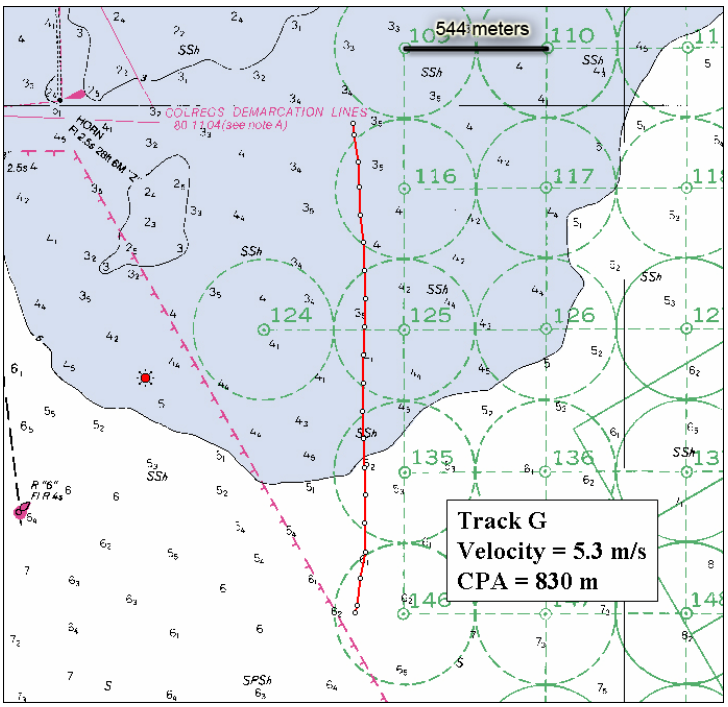

Figure 20. Track G.

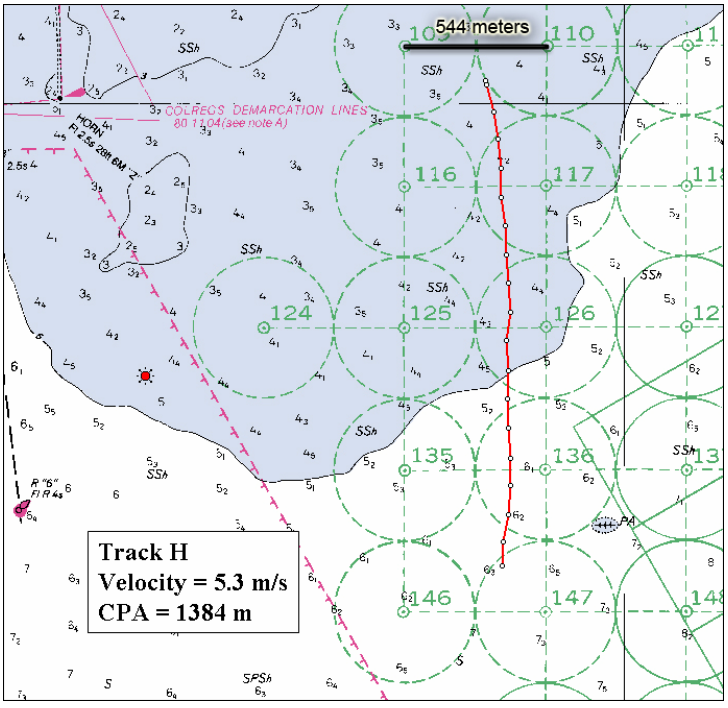

Figure 21. Track H.

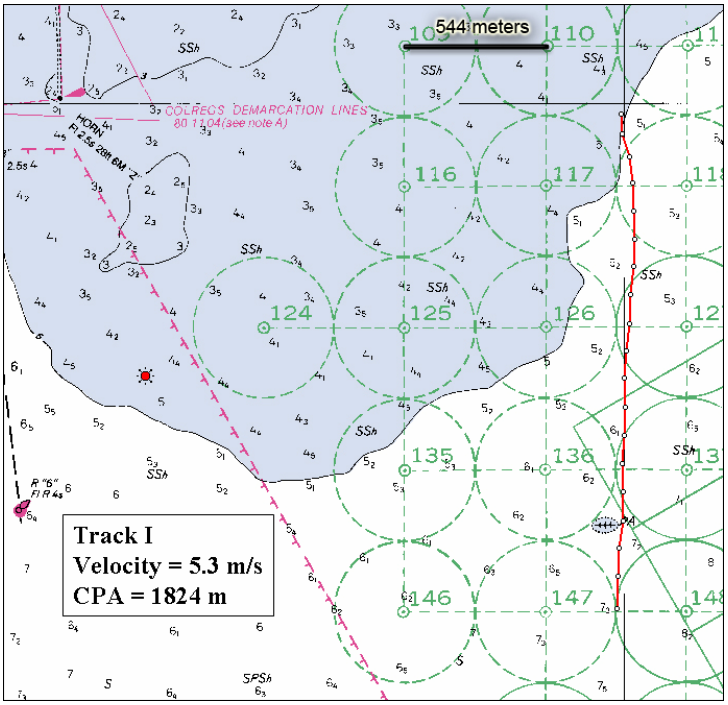

Figure 22. Track I.

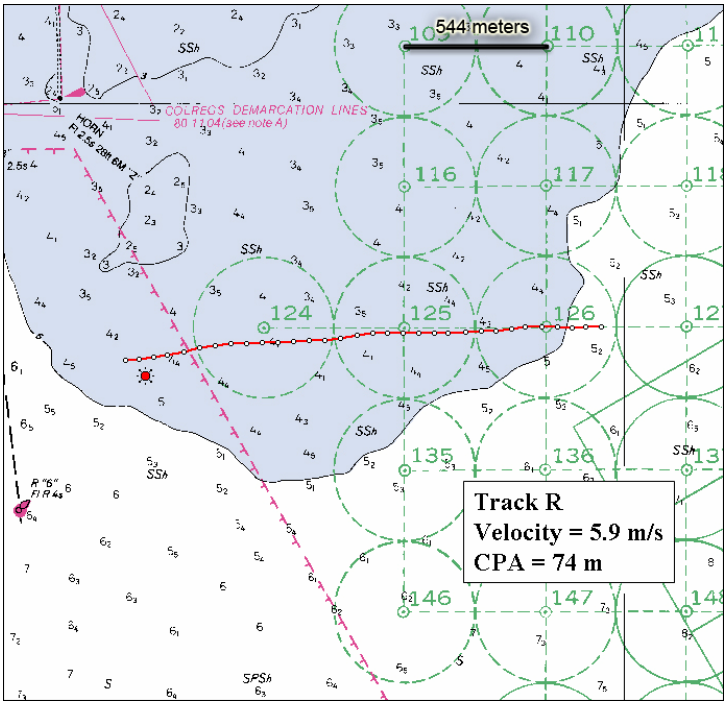

Figure 23. Track R (Radial Track).

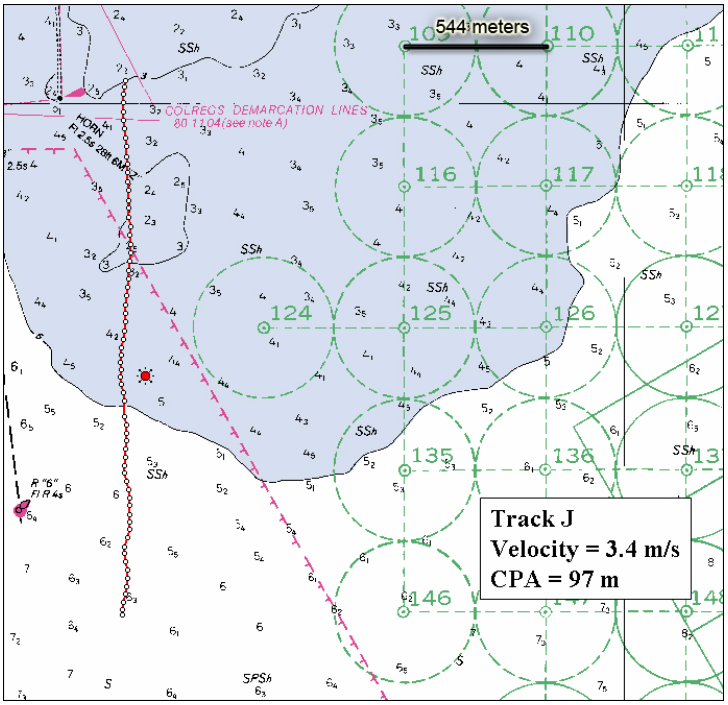

Figure 24. Track J.

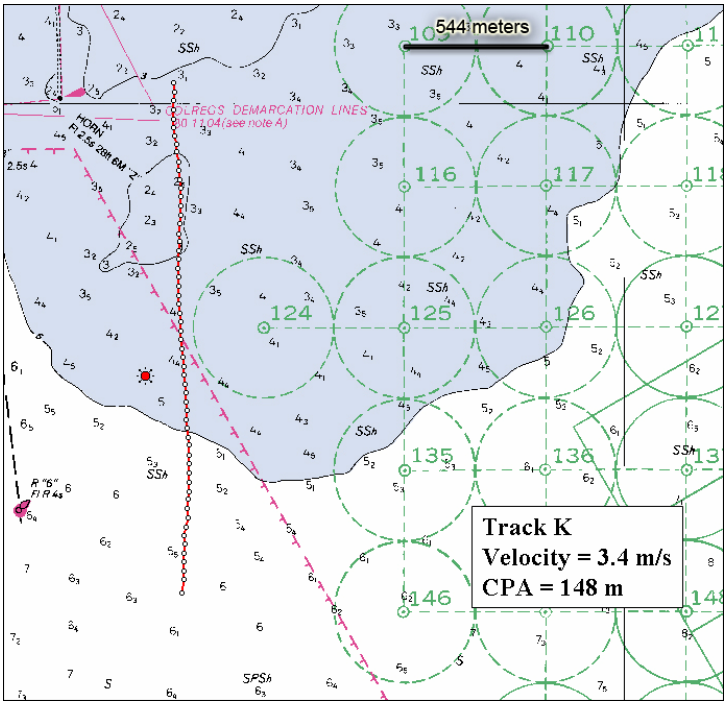

Figure 25. Track K.

IV. DATA ANALYSIS

A. PROCEDURE AND OVERVIEW

At the shore station, the acoustic time series corresponding to each track were stored as a .wav file. Using Spectrogram Version 11.0[1], the acoustic data are displayed as spectrograms . Using the "analyze file" function, the spectrogram is examined for the presence of Lloyd's mirror patterns and narrowband tonals.

Initial analysis of the data set involves zooming on the areas of the spectrogram which offer the most discernable frequency striations and narrowband tonals. Once the desired features of the spectrogram are highlighted to within ±1.4Hz, the highest resolution offered by the program, the cursor is used to retrieve pairs of frequency and time representing a frequency striation or tonal.

Using the equations developed and presented in Chapter II, these frequency and time pairs yield range and speed solutions for the target boat at CPA. This procedure is applied to each data set in which there is a usable Lloyd's mirror pattern corresponding to the target track. The estimated ranges and speeds are then compared to the ground truth for that track.

Part B of Chapter IV analyzes the data set corresponding to Track A and details the procedures used to estimate speed and range. Since the same analysis is applied to each track, Part C summarizes the results for the remaining tracks without showing the calculations.

[1] Copyright 2004, Visualization Software LLC.

B. TRACK A

1. Measuring *df* / *dt*

Figure 26 is the Lloyd's mirror interference pattern produced by the target as it passed through CPA for Track A. CPA from the target to the receiver is determined to be 54 meters using the GPS truth data. Average target speed of 5.6 m/s is measured by dividing the track length by the time required to complete the track.

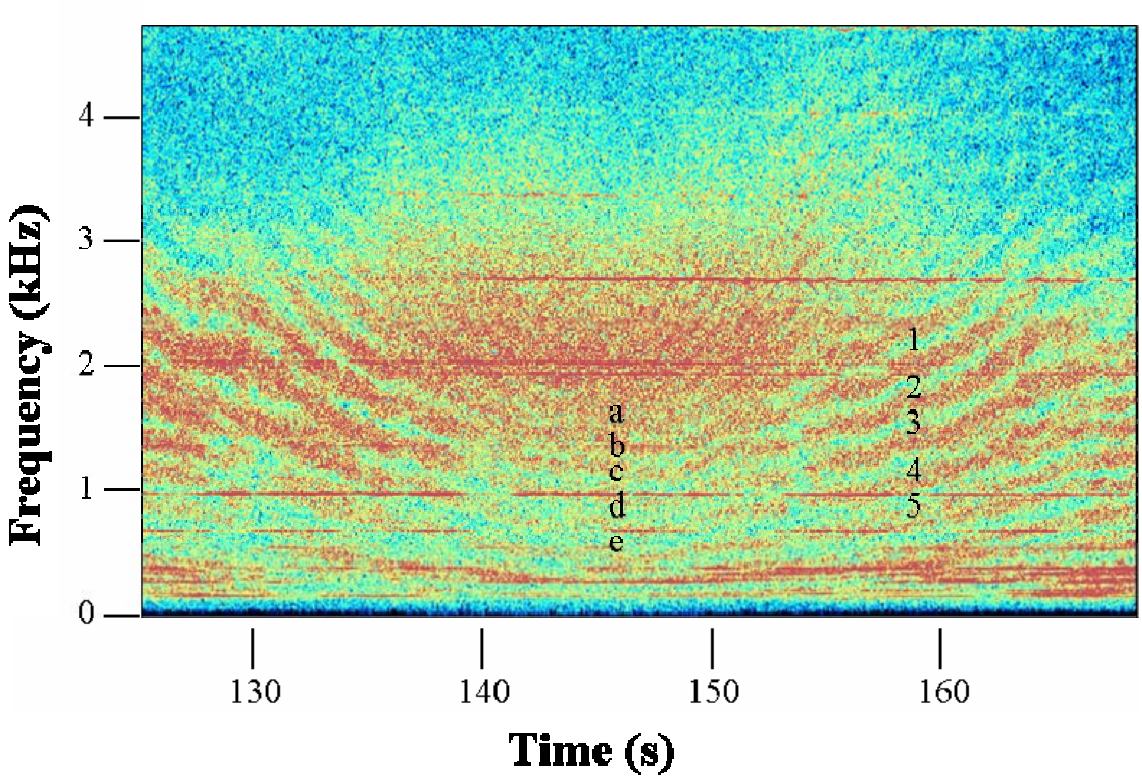

Figure 26. Lloyd's mirror interference pattern at CPA-Track A.

The number labels assigned to striations have no special significance. They are arbitrarily assigned as a means of matching frequency and time pairs to the appropriate striation. The criteria for analysis is that the striation must be clear enough and straight enough over at least a 5-second time period so that a representative value of df/dt can be obtained from the spectrogram.

The spectrogram is zoomed to an analysis band containing the striation of interest, thereby increasing the resolution and reducing the error in the measurements of the frequency time pairs. Figure 27 is a magnification of striation 1 from 156-162 seconds and 2030-2800 Hz. The black dots along the striation show where the individual frequency-time measurements are made. Table 3 lists corresponding frequency-time pairs and a resulting value of df/dt for striation 1 is $114.3\,\mathrm{sec}^{-2}$.

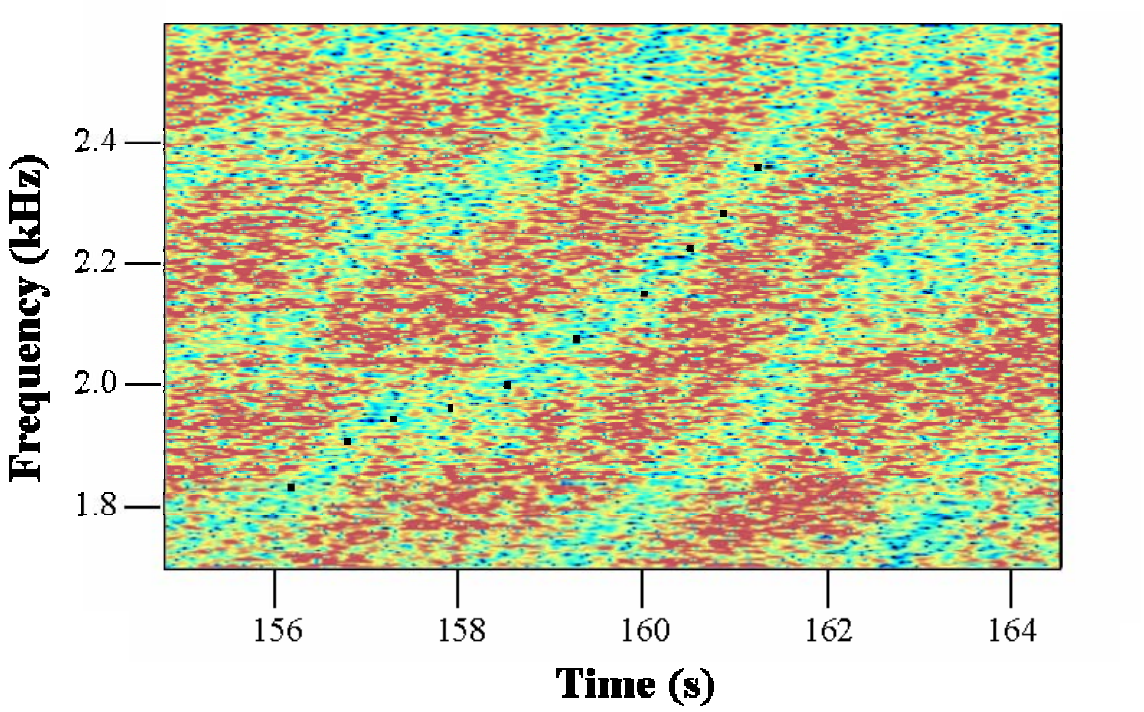

Figure 27. Track A striation 1.

Frequency (Hz)	1874	1934	1966	2052	2095	2192	2241	2359	2418	2504
Time (ms)	157.1	157.6	158.2	159.0	159.8	160.4	161.0	161.5	162.0	162.3

Table 3. Frequency-time pairs for Track A striation 1

This procedure is repeated for each designated striation in the spectrogram. The null frequencies, f_n, are located on the spectrogram where the target is at CPA and are designated a-e. Values of df/dt and the null frequencies f_n are tabulated for Track A in Table 4.

Striation	f_n (Hz)	df / dt ($\sec^{-2}$)
1	1314	114.3
2	1093	94.5
3	883	77.7
4	630	60.7
5	425	36.9

Table 4. Null frequencies and df / dt for Track A.

2. Measuring Target Speed

In Figure 26, the thin horizontal lines of high spectral energy which lay horizontally across the Lloyd's mirror interference pattern are narrowband tonals emitted by the target boat. As shown in Chapter II, the Doppler shift of the tonals as the target passes through CPA can be exploited to estimate target speed. This section details the procedure for estimating target speed on Track A.

In Figure 28, Track A's spectrogram has been zoomed so that the Doppler shift of a 1-kHz tonal is visible.

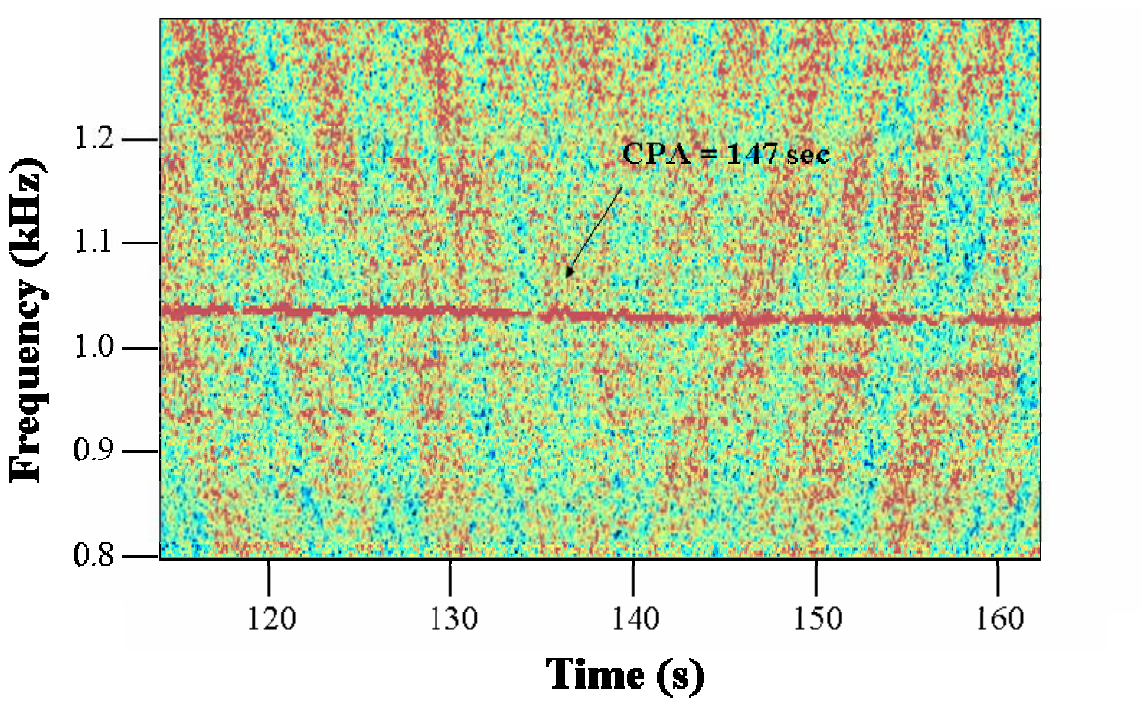

Figure 28. Tonal of the target boat passing through CPA.

Guided by the axis of the Lloyd's mirror parabola, the CPA time is 147 seconds. Using the cursor, the tonal frequency is measured on each side of CPA to determine the upper and lower frequencies, f_u and f_l. Applying equations (2.6)-(2.8) and using a sound speed at the receiver of 1516 m/sec from Figure 7, target speed is determined to be 5.6 m/s with a standard deviation of 1.0 sec. This estimate is compared to the ground-truth velocity of 5.6 m/s. This method is applied to each observable tonal above 1 kHz in the spectrogram. The results for track A are displayed in Table 5.

f_u (Hz)	f_l (Hz)	f_o (Hz)	Δf (Hz)	V (m/s)	V actual (m/s)
3566	3553	3559.5	13	5.54	5.63
2851	2840	2845.5	11	5.86	5.63
2140	2133	2136.5	7	4.97	5.63
2051	2043	2047.0	8	5.92	5.63
1424	1419	1421.5	5	5.33	5.63
1022	1018	1020.0	4	5.95	5.63

Table 5. Target speeds calculated using the Doppler shift.

3. Measuring Range at CPA

Now that the speed of the target is estimated, using the geometry from Figure 5 as a reference, equations (2.11) and (2.12) are used to calculate the range of the target as it passes through CPA. A separate CPA calculation is completed for each numbered striation. Table 6 shows the CPA ranges determined from each numbered striation. The average CPA range estimate is 56 meters with a standard deviation of 4 meters.

Striation	f_n (Hz)	$\frac{df}{dt}$ ($\sec^{-2}$)	v (m/s)	R_o (m)	R_o actual (m)
1	1314	114.3	5.6	58	54
2	1093	94.5	5.6	59	54
3	883	77.7	5.6	54	54
4	630	60.7	5.6	51	54
5	425	36.9	5.6	58	54

Table 6. CPA range using two-path ray theory.

C. OTHER TARGET TRACKS

1. Track B

Track B is a northbound track with CPA from the target boat to the receiver of 97 meters and target speed of 5.8 m/sec. Figure 29 is the broadband interference pattern and narrowband tonals produced by the target as it passes through CPA.

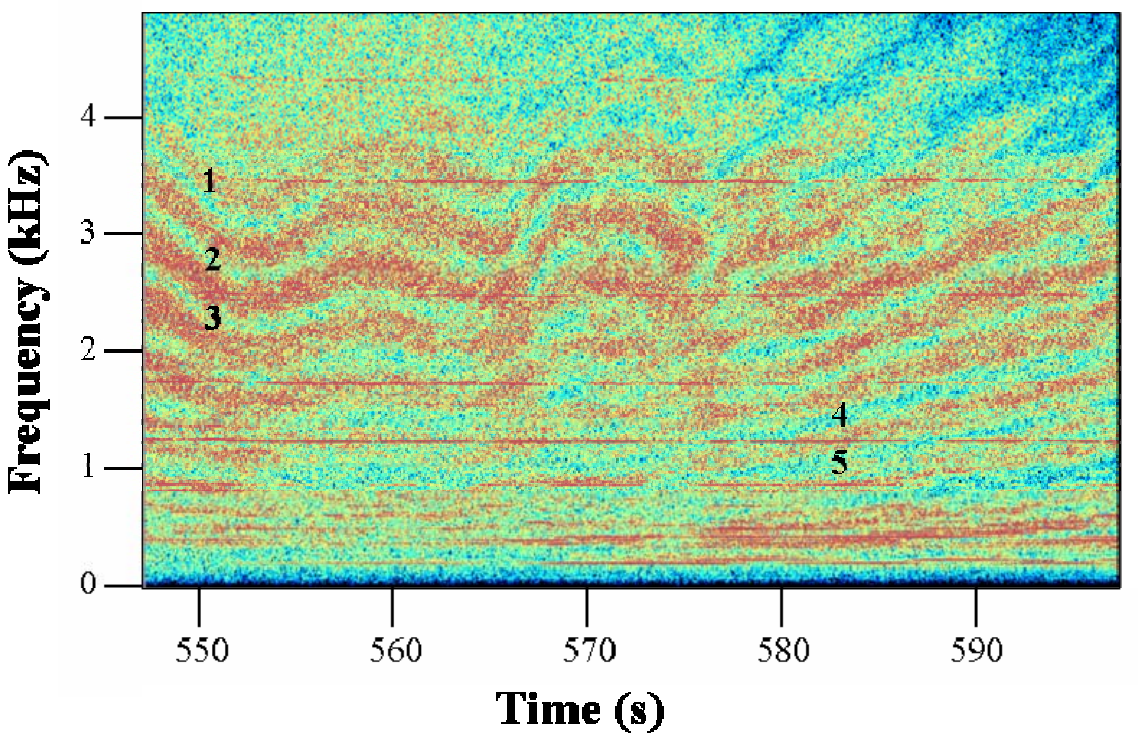

Figure 29. Broadband interference pattern corresponding to Track B.

f_u (Hz)	f_l (Hz)	f_o (Hz)	Δf (Hz)	V (m/s)	V actual (m/s)
3530	3519	3524.5	11	4.73	5.85
2830	2818	2824.0	12	6.44	5.85
2033	2026	2029.5	7	5.23	5.85
1414	1407	1410.5	7	7.52	5.85
1015	1012	1013.5	3	4.49	5.85

Table 7. Target speeds calculated using the Doppler shift.

Average speed of the target is 5.7 m/s with a standard deviation of 1 m/s. Using the average speed of 5.7 m/s, the range to the buoy at CPA is summarized in Table 8.

Striation	f_n (Hz)	$\frac{df}{dt}$ $\sec^{-2}$	v (m/s)	R_o (m)	R_o actual (m)
1	2833	168.6	5.7	95	97
2	2442	142.5	5.7	96	97
3	2011	132.3	5.7	84	97
4	768	42.6	5.7	96	97
5	725	36.7	5.7	107	97

Table 8. CPA range using two-path ray theory.

Average range for this data set is 95 meters with a standard deviation of 8 meters. It should be noted that in this data set, striations 1, 2, and 3 are taken on the side of the spectrogram where the target is closing. This is done because the striation slope is more linear on this side for the higher frequencies. This has no effect on the outcome because as long as the target maintains constant course and speed, the striation slopes are the same on either side of CPA.

There is a significant difference in the bathtub pattern produced by the target on Track B as compared to Track A. In Figure 29, instead of a perfectly hyperbolic Lloyd's mirror pattern, a wavy feature is present in the striations near CPA. A candidate hypothesis for this phenomenon is the effect of the sea state on the target boat. As mentioned in the environmental section, the wave interval was approximately 5 seconds with seas coming from the southwest. Track A, run on a southerly course was headed into the seas while track B, run on a northerly course, had a following sea which decreased maneuverability and caused the target to ride with the seas. As the target rode the crests and troughs of the waves, the depth of the source was modulated by the sea-surface waves. Upon inspection of the waves in the striations of the spectrogram, it appears they have a period of around 5 seconds which corresponds to the period of the waves experienced during the experiment.

2. Track C

Track C was a southbound track with a CPA from the target boat to the receiver of 185 meters and target speed of 5.9 m/s. Figure 30 shows the broadband interference pattern and narrowband tonals produced by the target boat as it passes through CPA.

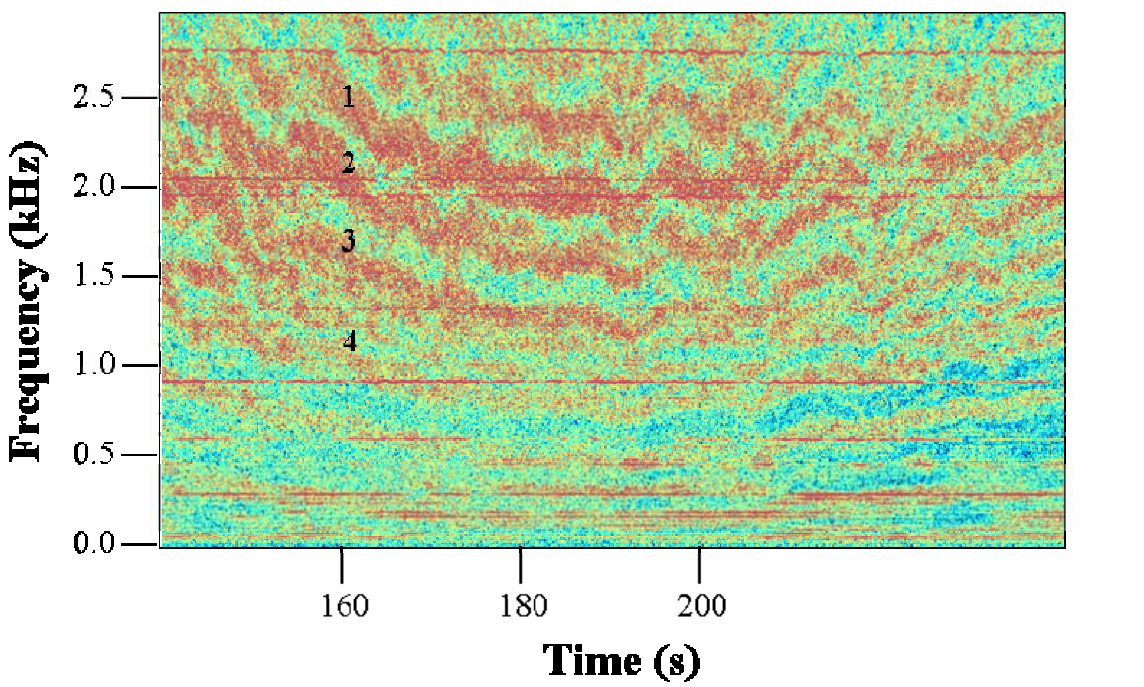

Figure 30. Broadband interference pattern corresponding to Track C.

f_u (Hz)	f_l (Hz)	f_o (Hz)	Δf (Hz)	V (m/s)	V actual (m/s)
3491	3480	3485.5	11	4.78	5.95
2790	2778	2784.0	12	6.53	5.95
2092	2083	2087.5	9	6.54	5.95
2006	1999	2002.5	7	5.30	5.95
1002	998	1000.0	4	6.06	5.95

Table 9. Target speeds calculated using the Doppler shift.

Average speed of the target is 5.8 m/s with a standard deviation of 1.0 m/s. Using the average speed of 5.8 m/s the range to the buoy at CPA is summarized in Table 10.

Striation	f_n (Hz)	$\frac{df}{dt}$ $\sec^{-2}$	v (m/s)	R_o (m)	R_o actual (m)
1	2117	77.1	5.8	160	185
2	1772	72.0	5.8	143	185
3	1433	49.3	5.8	170	185
4	711	22.4	5.8	186	185

Table 10. CPA range using two-path ray theory.

The average range calculated for this track is 165 meters with a standard deviation of 18 meters. The larger error associated with the analysis of Track C stems from inaccuracies in the calculation of df / dt as a result in the degradation of the Lloyd's mirror pattern. As the range between the target and the receiver increases, the energy received from the direct path and surface reflected path begin to lose coherence, leading to the interference pattern to become less stable.

3. Tracks D-I

For the remainder of the high-speed tracks, the Lloyd's mirror interference pattern transitioned from barely discernable to non-existent. The narrowband tonals also weaken and disappear with increasing target range. Nevertheless, in each spectrogram, it is evident that a target is present by the large amount of broadband energy. However, the techniques described in this thesis do not distinguish between the controlled target and other shipping.

4. Radial Track

The final high-speed track was an inbound radial track. Once the target boat completed Track I, it came about and traveled north until the buoy was on a bearing of 270 degrees relative as determined by the GPS waypoint taken when the buoy was initially launched. At the start of the Radial Track, the target turned toward the buoy and closed at 5.9 m/s. CPA to the buoy on the radial track was 73 meters. The intent of this track was to come as close to the buoy as possible. However, a close approach was

impeded by the watch circle created by the scope of the sonobuoy anchor line and poor visibility as it rode the waves. Figure 31 is the spectrogram of the radial track as the boat passed through CPA.

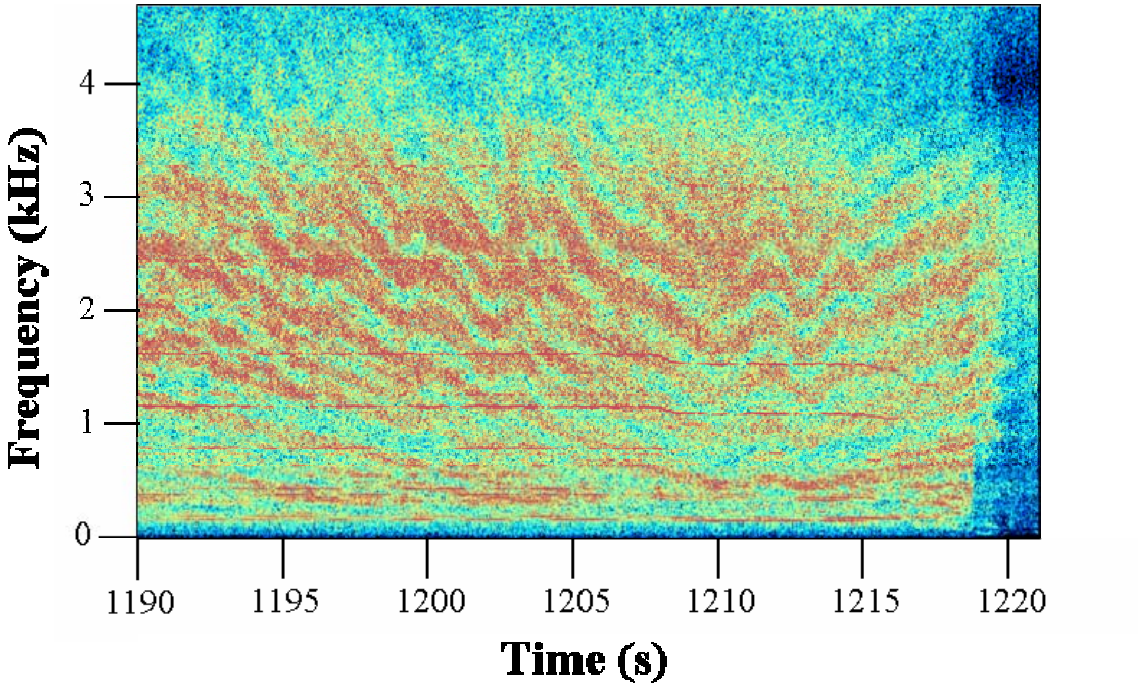

Figure 31. Spectrogram of Track R (Radial Track).

Two features of this spectrogram are immediately apparent. First is the sudden drop in spectral energy at 1220 seconds caused by the boat coming to a complete stop. Second are the very abrupt Doppler shifts present at 1197 seconds and 1212 seconds. These sudden Doppler shifts are caused by the boat abruptly throttling down. Even though the Radial Track produced very clear striations, the analysis methods assume a constant course and speed through CPA. As a result, estimation of range and speed for the Radial Track is impossible using two-path ray theory.

5. Track J

Track J is the first of two slower speed tracks. The ground truth CPA range is 97 meters and target velocity is 3.5 m/s. The first noticeable feature of the spectrogram produced by this track is the absence of several of the tonals present in the higher speed tracks. As the speed of the target decreased, certain tonals seem to disappear. This

supports the notion that the tonals produced by the target are frequencies which are excited by the operation of the propulsion and auxiliary equipment.

Another difficulty associated with the slower speed tracks was calculating the Doppler shift. The slower speed makes accurate calculation of Doppler shift difficult. Since further processing of the spectrogram to recover range at CPA requires an accurate speed derived from the Doppler shift, the range estimation is difficult as well. Figure 32 shows the spectrogram produced by the target on Track J.

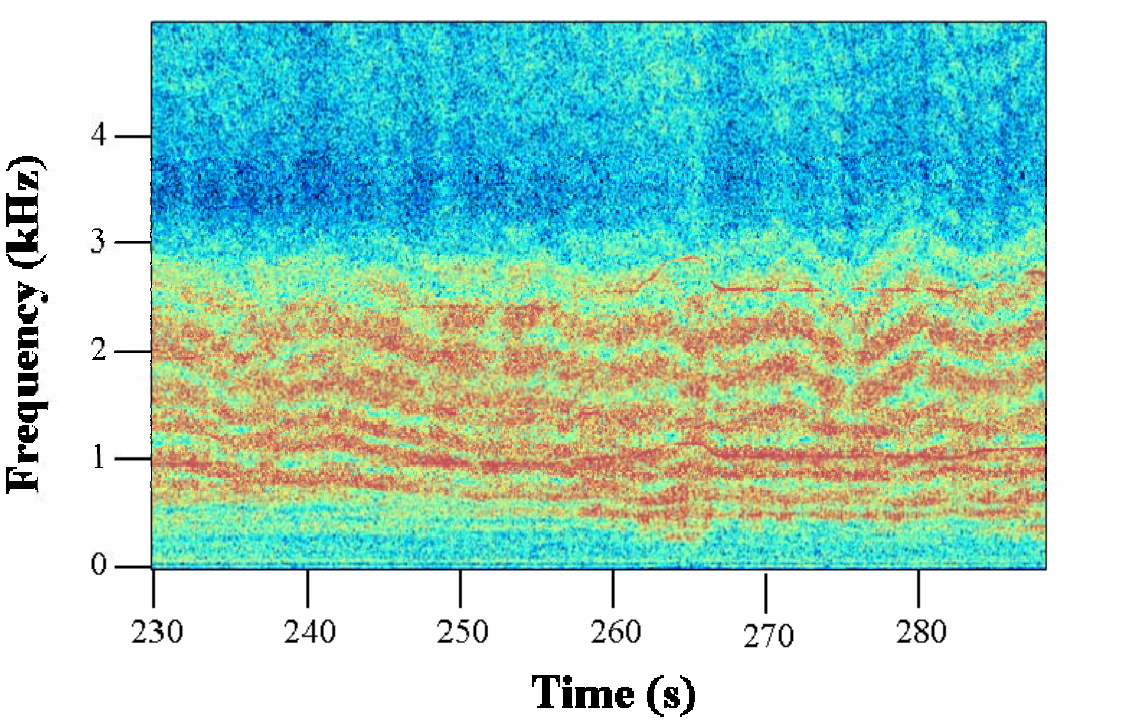

Figure 32. Spectrogram of Track J.

6. Track K

This was the last track of the experiment. Ground truth CPA was determined to be 148 meters with an average velocity of 3.4 m/s. Figure 33 is the broadband spectrogram and the tonals produced as the boat passed through CPA.

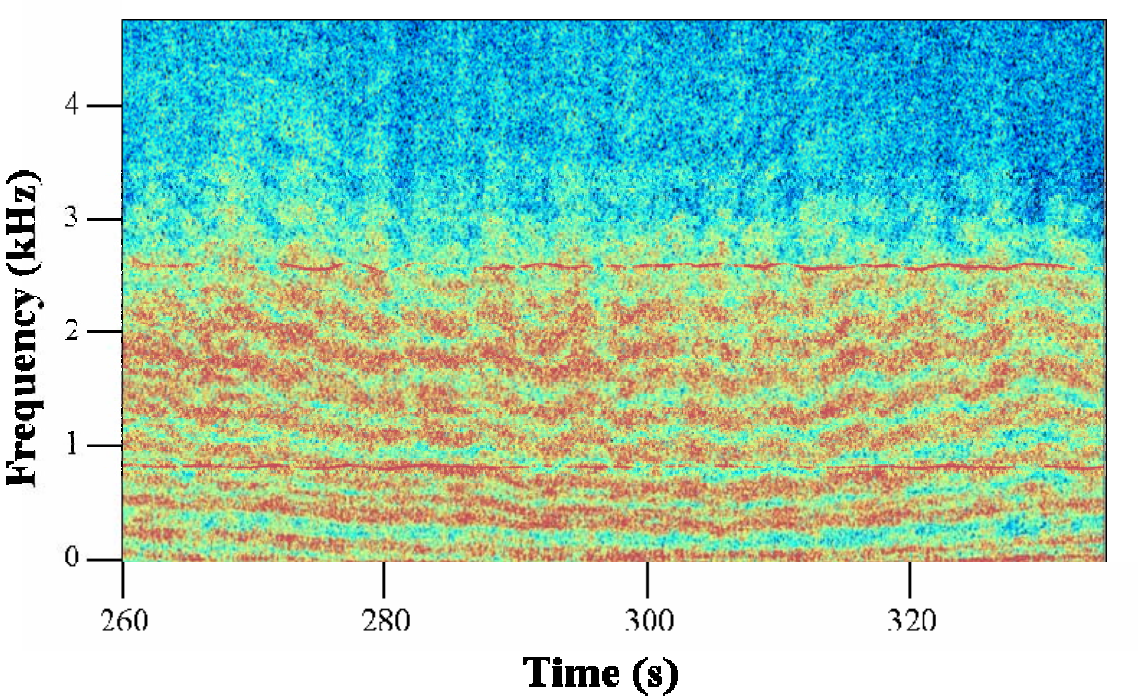

Figure 33. Spectrogram of Track K.

Only the tonal at 1200 Hz is capable of being analyzed. The speed calculated by the Doppler shift of the tonal at 1200 Hz is 1.3 m/s. Using this speed the CPA ranges are calculated and presented in Table 11.

Striation	f_n (Hz)	$\frac{df}{dt}$ ($\sec^{-2}$)	v (m/s)	R_o (m)	R_o actual (m)
1	2305	63.85483	1.3	45	148
2	2031	66.95328	1.3	38	148
3	1734	59.02933	1.3	36	148
4	1417	38.27771	1.3	46	148
5	1115	40.03208	1.3	35	148
6	840	22.47044	1.3	47	148
7	528	16.11198	1.3	41	148

Table 11. CPA range using two-path ray theory.

The average CPA range is 41 meters with a standard deviation of 5 meters. This poor range estimate results from the inability to determine the speed from the Doppler shifts in the spectrogram. Due to the long range and slow speed of the source, Δf in equation (2.7) is not large enough to produce an accurate calculation of target speed.

V. CONCLUSIONS AND RECOMMENDATIONS

A. CONCLUSIONS

1. The Waveguide Invariant and Two-path Ray Theory

Chapter II shows how the waveguide invariant theory reduces to the same equations as those predicted by an isovelocity two-path ray model for estimating range and speed of a source traveling at constant course and speed through CPA. When β=1, the two methods yield identical results.

Using the isovelocity two-path model, target range at CPA is accurate to within 9% at ranges of 185 meters. The ability to exploit the Lloyd's mirror interference pattern is highly dependent on the sea state, target range and target speed. A rough sea surface and increased target range led to loss of coherence in the surface reflected path. The resulting interference pattern is distorted and weakened, hindering accurate determination of df/dt. Changes in target speed at or near CPA create large fluctuations in the narrowband tonals and produce inaccurate speed estimates. Additionally, slower target speeds coincide with lower signal levels, making it difficult to estimate Doppler shifts in the narrowband signal components.

2. Zuniga `07

The Zuniga experiment provided an excellent test for the concept of using single hydrophones laid out in a maritime sensing network to track sources in the shallow-water coastal regions that have become so significant in naval operations. The oceanographic features and ship traffic at this site were representative of environments in which such systems are likely to be deployed. In terms of the fitting the theoretical assumptions used to derive the various estimates, the site was certainly not ideal. The environment was noisy because of the sea state and shipping. The development of the Lloyd's mirror pattern is contingent on the sea surface being smooth enough to support a reflected surface path. Nevertheless, even with the rough seas experienced during the experiment,

the channel did support the formation of Lloyd's mirror patterns which enabled CPA range and speed predictions out to 185 yards.

In several of the spectrograms there appears to be a "waviness" associated with the Lloyd's mirror pattern. Track B shows a clear example of this phenomenon. Looking at equation (2.3), as the boat is closing and opening CPA, the only thing which changes is the depth of the source as it rides up and down the waves. Looking at the time interval of the waves in the striation, the waves appear with about a 5-second period, which corresponds to the seas observed during the test.

3. Limitations of Theory

For both the waveguide invariant and two-path ray theory methods, the target must maintain constant course and speed through CPA. As was seen in the radial track, any speed variation close to CPA affects the tonals, hindering the use of Doppler for speed and range calculations.

Mitigating this issue is the availability of multiple distributed sensors forming the deployed sensor network. The modem spacing provides multiple opportunities to catch a target which is steady on course and speed. If a speed or course perturbation created by the target vessel has a negative effect on the tracking solution produced by the first modem, then by the time it reaches the next modem it may be steady on course and speed and therefore susceptible to being tracked.

The range and speed estimates for Tracks A and B had mean values extremely close to ground truth with small standard deviations. As was seen in the CPA's which exceed 185 meters, the distortion of the Lloyd's mirror pattern hindered analysis using the two methods. Had the sea state been more benign, range and speed analysis may have been possible for some of the longer range tracks as well. However, in the context of the maritime surveillance scenario in which these modems would be deployed, the effective range achieved in this experiment is operationally useful. Moreover, although tracks D-I do not produce usable spectrograms, there is significant broadband energy corresponding to the target which could be exploited for detection.

B. POTENTIAL FOLLOW-ON RESEARCH

Although Zuniga`07 proves that detections and resolution of target kinematics are possible, it is recommended that the experiment, be repeated in near ideal environmental conditions. This would establish an upper bound for expected ranges determined by these methods. Resolution of target kinematics using these methods would need to be automated providing further opportunities for follow-on research. Additionally, if the sensor system was to be deployed in a very narrow channel or harbor, two-path ray theory can easily be applied to situations where the range is not large compared to source and receiver depth. Further physics-based research could investigate the waviness feature present in many of the spectrograms and explain the effects of sea-state, bathymetry and bottom type.

Zuniga `07 was a controlled experiment where the target's location was known at all times. In an operational setting, it will be necessary to distinguish between contacts of interest and other shipping. Further development of this capability will require a means to isolate desired targets and ignore those of no tactical value.

If it is desired for an underwater acoustic modem to estimate target range and CPA, the methods described in this thesis are readily implemented in software for operation on the modem. Zuniga`07 could be repeated using an undersea modem configured to receive the acoustic energy of a surface target. Since the theory regarding the development of target range and CPA has been validated, a follow on test would identify any possible issues which exist with the modem which would preclude it from being a good passive sensor. Further experiments could test the validity of the approach against a wide variety of targets.

Once complete, follow on experiments could develop the detection and reporting capabilities of a complete modem network, from detection to reporting.

THIS PAGE INTENTIONALLY LEFT BLANK

LIST OF REFERENCES

Brekhovskikh, L. M., and Lysanov, Y. P. *Fundamentals of Ocean Acoustics, 3rd Edition.* New York: Springer-Verlag, 2003, pp. 140-146.

D`Spain, Gerald, and Kuperman, William A. "Application of waveguide invariants to analysis of spectrograms from shallow water environments that vary in range and azimuth." *The Journal of the Acoustical Society of America* 106 (1999), pp. 4966-4999.

Kapolka, Daphne. *Underwater Acoustics for Naval Applications,* Course notes, Naval Postgraduate School (2007) Chapter IV, pp. 2-7.

Kuperman, William A., D`Spain, Gerald, Song, Hee Chung and Thode, Aaron. "The Generalized Waveguide Invariant Concept with Application to Vertical Arrays in Shallow Water," Ocean Acoustic Interference Phenomena and Signal Processing, *AIP Conference Proceedings* 621 (2001), pp. 33-37.

Lee, Sunwoong and Makris, Nicholas C. "The array invariant," *The Journal of the Acoustical Society of America,* 119 (2006) pp. 336-351.

National Strategy for Combating Terrorism, 11 September 2006, accessed 12 August 2006, at http://www.whitehouse.gov/nsc/nsct/2006/, pp. 9-13.

Rouseff, Daniel and Leigh, Charlotte. "Using the Waveguide Invariant to Analyze Lofargrams," *Oceans 2002 MTS/IEEE*, 4 (2002), pp. 2239-2243.

Urick, Robert. *Principles of Underwater Sound 3rd Edition*. Los Altos: Peninsula Publishing, 1996, pp. 128-131.

THIS PAGE INTENTIONALLY LEFT BLANK

INITIAL DISTRIBUTION LIST

1. Defense Technical Information Center
   Ft. Belvoir, VA

2. Dudley Knox Library
   Naval Postgraduate School
   Monterey, CA

3. Professor Joseph Rice
   Naval Postgraduate School
   Monterey, CA

4. CDR Denise Kruse
   Naval Postgraduate School
   Monterey, CA

5. Professor Daphne Kapolka
   Naval Postgraduate School
   Monterey, CA

6. Professor Kevin Smith
   Naval Postgraduate School
   Monterey, CA

7. Professor Donald Brutzman
   Naval Postgraduate School
   Monterey, CA

8. RADM (Ret) Ray Jones
   Naval Postgraduate School
   Monterey, CA

9. RADM (Ret) Rick Williams
   Naval Postgraduate School
   Monterey, CA

10. Wendy Walsh
    Naval Postgraduate School
    Monterey, CA

11. Paul Hursky
    Heat, Light, and Sound
    San Diego, CA

12. Bill Marn
SPAWAR Systems Center
San Diego, CA

13. Doug Grimmett
SPAWAR Systems Center
San Diego, CA

14. Bob Creber
SPAWAR Systems Center
San Diego, CA

15. Lonnie Hamme
SPAWAR Systems Center
San Diego, CA

16. Dr. Suzanne Huerth
SPAWAR Systems Center
Charleston, SC

17. Tom Drake
Office of Naval Research
Washington, DC

18. Dana Hesse
Office of Naval Research
Washington, DC

19. Captain Rick Ruehlin
Naval Sea Systems Command
Washington DC

20. LCDR Patrick Lafontant
Naval Sea Systems Command
Washington DC

21. Dr. Paul Gendron
Naval Research Laboratory
Washington DC

22. Jody Wood-Putnam
Naval Surface Warfare Center
Panama City, FL

23. Tony Matthews
Naval Surface Warfare Center
Panama City, FL

24. Joel Peak
Naval Surface Warfare Center
Panama City, FL

25. Robert Mabry
US Special Operations Command
Tampa, FL

26. Andy Poole
US Special Operations Command
Tampa, FL

27. Shawn Martin
US Special Operations Command
Tampa, FL